International Journal of Thermophysics, Vol. 18, No. 5, 1997

Thermodynamic and Transport Properties of Fluids and Fluid Mixtures in the Extended Critical Region

S. B. Kiselev[1, 2] **and V. D. Kulikov**[1]

Received October 10, 1996

A practical representation of the thermodynamic properties and the transport coefficients related to diffusion, heat conduction, and their cross-processes in pure fluids and binary mixtures near the liquid–vapor critical line is developed. Crossover equations for the critical enhancement of those coefficients incorporate the scaling laws near the critical point and are transformed to the regular background far away from the critical point. The crossover behavior of the thermal conductivity and the thermal diffusion ratio in binary mixtures is also discussed. A comparison is made with thermal-conductivity data for pure carbon dioxide, pure ethane, and carbon dioxide add ethane mixtures.

KEY WORDS: binary mixtures; critical phenomena; carbon dioxide; diffusion coefficient; equation of state; ethane, fluid; specific heat; thermal conductivity; transport properties.

1. INTRODUCTION

It is well known that the state of a fluid near the critical point is characterized by anomalous large fluctuations of the order parameter [1, 2]. The intensity of these fluctuations diverges at the critical point. As a consequence, both the thermodynamic surface and the transport properties of fluids exhibit the singularities at the critical point. The asymptotic singular behavior of the thermodynamic properties and of the kinetic coefficients related to diffusion, heat conduction, and their cross-processes in binary mixtures can be described in terms of scaling laws with universal exponents and universal scaling functions [3–7]. However, the validity of these laws is restricted to, the near-vicinity around the critical point. On the other

[1] Institute for Oil and Gas Research of the Russian Academy of Sciences, Leninsky Prospect 63/2, Moscow 117917, Russia.

[2] To whom correspondence should be addressed.

0195-928X/97/0900-1143$12.50/0

hand, it has become evident that critical fluctuations are actually present in fluids over a very large range of temperatures and densities [8, 9]. In order to account for effects of these fluctuations on the equation of state and on the kinetic coefficients of fluids, it is necessary to consider the non-asymptotic critical behavior of the thermodynamic and transport properties including the crossover to regular classical behavior far away from the critical point. For one-component fluids this task is practically solved [8–14]. For binary mixtures the decoupled-mode calculations by Kiselev and co-workers [15–17], the recent renormalization-group calculations by Folk and Moser [18–20], and the mode-coupling results obtained by Luettmer-Strathmann and Sengers [21] not only confirm earlier asymptotic predictions, but also extend the description of the transport properties of binary mixtures into the crossover region. However, in Refs. 15–17 and 21 the thermodynamic properties for carbon dioxide and ethane mixtures were calculated from the crossover equation of state of Jin et al. [22, 23], which has been obtained without account of the new $C_{v,x}$ data obtained by Magee [24] and P, ρ, T, x data obtained by Lau [25] over a wide range of the temperatures and densities. Moreover, the crossover model proposed by Luettmer-Strathmann and Sengers [21] represents a fit of their crossover equations to experimental thermal-conductivity data at separate compositions and isochores only and cannot be used for the calculation of the transport properties of carbon dioxide and ethane mixtures on the entire thermodynamic surface.

It is the purpose of the present paper to describe the thermodynamic and transport properties of binary mixtures in a wide region around the critical point on the basis of the modern theory of critical phenomena. In calculating the thermodynamic properties for pure fluids and binary mixtures a new parametric crossover equation of state which incorporates the scaling laws asymptotically close to the critical point and transforms into the regular classical expansion far away from the critical point has been used [26]. In evaluating the crossover expressions for the kinetic coefficients in binary mixtures we use the decoupled-mode theory method originally introduced by Ferrell [27]. The crossover equations for the critical enhancements of the transport coefficients is developed by incorporating a finite cutoff wave number and time-dependent correlation functions of the order parameter and the entropy into the decoupled-mode theory integrals. This study has led us to introduce some modifications in the simple crossover model obtained earlier by Kiselev and Kulikov [15]. It is shown that the correct regular behavior of the transport coefficients is provided by the redefinition of the correlation length of the order-parameter fluctuations. In the vicinity of the critical point the crossover expressions for the critical enhancements of the transport coefficients in a

binary mixture incorporate the scaling laws and reproduce the asymptotic expressions obtained earlier by Mistura [4, 5]. Far away from the critical point the crossover expressions transform into their regular background parts. The crossover expressions for the thermal conductivity and the thermal-diffusion ratio in binary mixtures are also considered.

We proceed as follows. In Section 2, we formulate the crossover equations for the Onsager kinetic coefficients. In Section 3, we analyze on this basis the crossover behavior of the thermal conductivity and the thermal-diffusion ratio near the liquid–vapor critical point of binary mixtures. A new parametric crossover equation of state for mixtures of carbon dioxide and ethane and a comparison with experimental data in the one- and two-phase regions are discussed in Section 4. In Section 5, we discuss the role of the regular (background) parts of the kinetic coefficients in the crossover behavior of the thermal conductivity of mixtures and propose simple expressions for calculating these coefficients in mixtures of carbon dioxide and ethane. A comparison with experimental thermal-conductivity data for pure carbon dioxide, pure ethane, and carbon dioxide and ethane mixtures in the critical region is given in Section 6. In Section 7, we discuss our results.

2. CROSSOVER EQUATIONS FOR THE KINETIC COEFFICIENTS

The Onsager expressions for the diffusion current $\vec{J}_d$ and heat current $\vec{J}_q$ in binary mixtures read [28]

$$\vec{J}_d = -\tilde{\alpha}\,\nabla\mu - \tilde{\beta}\,\nabla T \tag{1}$$

$$\vec{J}_q = -\tilde{\beta} T\,\nabla\mu - \tilde{\gamma}\,\nabla T + \mu\vec{J}_d \tag{2}$$

where T is the temperature, $\mu = \mu_2 - \mu_1$ is the chemical potential of the mixture, and $\tilde{\alpha}$, $\tilde{\beta}$, and $\tilde{\gamma}$ are Onsager kinetic coefficients. Mode-coupling calculations performed by Gorodetskii and Giterman [3] and Mistura [4, 5] show that, asymptotically close to the critical point, the Onsager kinetic coefficients diverge as the thermal conductivity of a one-component fluid,

$$\Delta\tilde{\alpha} = \tilde{\alpha} - \tilde{\alpha}_b = \frac{k_B T \rho}{6\pi\eta\xi}\left(\frac{\partial x}{\partial \mu}\right)_{P,T} \tag{3}$$

$$\Delta\tilde{\beta} = \tilde{\beta} - \tilde{\beta}_b = \frac{k_B T \rho}{6\pi\eta\xi}\left(\frac{\partial x}{\partial T}\right)_{P,\mu} \tag{4}$$

$$\Delta\tilde{\gamma} = \tilde{\gamma} - \tilde{\gamma}_b = \frac{k_B T \rho}{6\pi\eta\xi}\left(\frac{\partial S}{\partial T}\right)_{P,\mu} \tag{5}$$

where η is the shear viscosity, ρ the density, $x = N_2/(N_1 + N_2)$ the mole fraction of the second component, S the molar entropy of the mixture, ξ the equilibrium correlation length, k_B Boltzmann's constant, and the subscript "b" denotes the background part of the kinetic coefficients, which is an analytic function of the concentration, temperature, and density. The asymptotic equations, Eqs. (3)–(5), are valid only over an extremely small range of temperatures and densities around the critical point. In order to consider the crossover behavior of the transport coefficient in binary mixtures, it is convenient to start from the correlation-function expressions also known as "Kubo formulas,"

$$\tilde{\alpha} = \frac{1}{6k_B T} \int d\vec{r} \int dt \langle \vec{J}_d(0, 0)\, \vec{J}_d(\vec{r}, t) \rangle \tag{6}$$

$$\tilde{\beta} = \frac{1}{6k_B T^2} \int d\vec{r} \int dt \langle \vec{J}_d(0, 0)\, \vec{J}_S(\vec{r}, t) \rangle \tag{7}$$

$$\tilde{\gamma} = \frac{1}{6k_B T^2} \int d\vec{r} \int dt \langle \vec{J}_S(0, 0)\, \vec{J}_S(\vec{r}, t) \rangle \tag{8}$$

where $\vec{J}_d$ and $\vec{J}_S$ are the microscopic diffusion and heat currents. Since the concentration and entropy density are slow variables near a critical point, they may treated as independent from the velocity fluctuations in the current–current correlation functions. If $\vec{J}_d = \rho\, \delta x \vec{v}$ and $\vec{J}_S = T\rho\, \delta S \vec{v}$ (where δx and δS denote the deviations of concentration and local entropy from the equilibrium values, and $\vec{v}$ is a velocity), Eqs. (6)–(8) transform to

$$\Delta\tilde{\alpha} = \frac{\rho^2}{6k_B T} \int d\vec{r} \int dt \langle \delta x(0, 0)\, \delta x(\vec{r}, t) \rangle \langle \vec{v}(0, 0)\, \vec{v}(\vec{r}, t) \rangle \tag{9}$$

$$\Delta\tilde{\beta} = \frac{\rho^2}{6k_B T} \int d\vec{r} \int dt \langle \delta x(0, 0)\, \delta S(\vec{r}, t) \rangle \langle \vec{v}(0, 0)\, \vec{v}(\vec{r}, t) \rangle \tag{10}$$

$$\Delta\tilde{\gamma} = \frac{\rho^2}{6k_B} \int d\vec{r} \int dt \langle \delta S(0, 0)\, \delta S(\vec{r}, t) \rangle \langle \vec{v}(0, 0)\, \vec{v}(\vec{r}, t) \rangle \tag{11}$$

Thus the correlation functions for the fluctuating currents have been factorized, which is referred to as the "decoupled-mode" approximation [27], by means of which the correlation functions become simply the products of the correlation functions of the individual fluctuating variables. In order to establish the behavior of the velocity correlations we may restrict ourselves

to linearized hydrodynamics equation. In this case we have, for the velocity–velocity correlation function [1, 28],

$$\langle \vec{v}(0,0)\,\vec{v}(\vec{r},t)\rangle = \frac{k_B T}{4\rho}\frac{1}{\sqrt{(\pi\nu t)^3}}\exp\left(-\frac{r^2}{4\nu t}\right) \tag{12}$$

with $\nu = \eta/\rho$, and where η is a high-frequency shear viscosity which is finite at the critical point [27]. Very close to the critical point the relaxation time of the fluctuations is extremely large, and in a zero-order approximation we may ignore the time dependence of the correlations of the concentration and entropy on the right-hand side of Eqs. (9)–(11) and replace them with the corresponding static correlation functions. With the Ornstein–Zernike approximation for the static correlation function of the order parameter

$$G(k) = \langle |\varphi_{\vec{k}}|^2\rangle = \frac{k_B T}{[1+(k\xi)^2]\,\rho}\left(\frac{\partial x}{\partial \mu}\right)_{P,T} \tag{13}$$

(where $\varphi_{\vec{k}}$ is a Fourier component of the order parameter at wave vector $\vec{k}$), Eqs. (9)–(11) with account of Eq. (12) are simply transformed into the asymptotic expressions for the kinetic coefficients in the form of Eqs. (3)–(5). In order to obtain the crossover expressions for the kinetic coefficients, the time-dependent correlation functions for the concentration and entropy in Eqs. (9)–(11) should be considered. Since at the critical point the most slowly relaxing variable is the order parameter, first we consider the time dependence of the order parameter. For the conserved order parameter the equation of motion has the form of a linear Langevin equation [2],

$$\frac{\partial\varphi(\vec{r},t)}{\partial t} = \frac{\tilde{\alpha}}{\rho^2}\nabla^2\left(\frac{\delta H}{\delta\varphi}\right) + \zeta(\vec{r},t) \tag{14}$$

where $\zeta(\vec{r},t)$ is a Gaussian noise source, and the effective Hamiltonian of the system near the critical point can be written in the Landau–Ginzburg form [1],

$$H = \int d\vec{r}\left[a\tau\frac{\varphi^2}{2} + \frac{c}{2}(\nabla\varphi)^2 + \frac{u}{4}\varphi^4\right] \tag{15}$$

where $\tau = T/T_c - 1$ is the dimensionless deviation of the temperature from the critical temperature T_c, and a, c, and u are positive constants. The term $\sim\varphi^4$ in Eq. (15) takes into account an interaction between fluctuations of

the order parameter. This term plays an essential role in the calculation of the critical exponents which determine the asymptotic scaling behavior of the thermodynamic properties of the system near the second-order phase transition. For this purpose it is necessary to apply the renormalization-group method [2], which makes Eq. (14) too complicated for the further analysis. As long as we are interested in simple crossover expressions connecting the thermodynamic and transport properties of binary mixtures, we consider the solution of Eq. (14) in the Gaussian approximation ($u=0$). However, in the final expressions we use for all thermodynamic quantities the scaled equations with the theoretical values of the critical exponents.

In terms of Fourier components, the solution of Eq. (14) reads

$$\delta\varphi_{\vec{k}} = \int_{-\infty}^{t} e^{-\tilde{\alpha}_{\vec{k}}\rho^{-2}k^2(a\tau + ck^2)(t-t')}\zeta_{\vec{k}}(t')\,dt' \tag{16}$$

which, together with the normalization

$$\langle \zeta_{\vec{k}}(t)\,\zeta_{\vec{k}'}(t')\rangle = 2k_B T\tilde{\alpha}_{\vec{k}}k^2\delta_{\vec{k},-\vec{k}'}\delta(t-t') \tag{17}$$

yields

$$\langle \delta\varphi_{\vec{k}}(0)\,\delta\varphi_{\vec{k}}(t)\rangle = G(k)\exp\left(-\frac{k_B T\tilde{\alpha}_{\vec{k}}k^2 t}{\rho^2 G(k)}\right)\delta_{\vec{k},-\vec{k}'} \tag{18}$$

where $G(k)$ is the Ornstein–Zernike correlation function as given by Eq. (13) with $\xi = \sqrt{c\rho^{-1}(\partial x/\partial\mu)_{P,T}}$ the correlation length in this approximation. Substitution of Eqs. (18) and (12) into Eq. (9) and integration over the variables $\vec{r}$ and t yield

$$\Delta\tilde{\alpha} = \frac{\rho}{12\pi^3}\int_0^{q_D} d\vec{k}\,\frac{G(k)}{k^2[\nu + k_B T\tilde{\alpha}_{\vec{k}}\rho^{-2}G^{-1}(k)]} \tag{19}$$

The integral is to be evaluated over all k up to the maximum cutoff wave number $q_D = |\vec{q}_D|$ first introduced by Pert and Ferrell [29]. The k-dependent transport coefficient $\tilde{\alpha}_{\vec{k}}$, similar to the transport coefficient $\tilde{\alpha}$, can be represented in the form

$$\tilde{\alpha}_{\vec{k}} = \Delta\tilde{\alpha}(k) + \tilde{\alpha}_b(k) = \Delta\tilde{\alpha}(k) + \tilde{\alpha}_b(0) \tag{20}$$

where we ignore the k dependence of the background part $\tilde{\alpha}_b(k)$ and consider it in the hydrodynamic limit $\tilde{\alpha}_b(k) = \tilde{\alpha}_b(0) = \tilde{\alpha}_b$. The transport coefficient

$$\Delta\tilde{\alpha}(k) = \Delta D(k)\,\rho\chi(k) \tag{21}$$

where we have introduced the notation $\chi(k) = (\partial x/\partial \mu)_{P,T}/(1 + k^2\xi^2)$. The k-dependent diffusion coefficient $\Delta D(k)$, similar to the thermal diffusivity $\Delta D_T(k)$ of the one-component fluids, in the asymptotic critical region in the limit $q_D \to \infty$ satisfies an equation of the form

$$\Delta D(k) = \frac{k_B T}{6\pi\eta\xi} \Omega_K(k\xi) \tag{22}$$

where $\Omega_K(z) = (\frac{3}{4}z^2)[1 + z^2 + (z^3 - z^{-1}) \arctan(z)]$ is the so-called Kawasaki function [30, 31]. Then Eq. (19), with account of Eqs. (13) and (22), reads

$$\Delta\tilde{\alpha} = \frac{k_B T\rho}{6\pi\eta\xi} \left(\frac{\partial x}{\partial \mu}\right)_{P,T} \Omega_x(q_D\xi) \tag{23}$$

where

$$\Omega_x(q_D\xi) = \frac{2}{\pi} \int_0^{q_D\xi} \frac{dz}{\left[(1+z^2)\left(1 + \frac{\tilde{\alpha}_b}{\eta}\left(\frac{\partial \mu}{\partial x}\right)_{P,T} [1 + y_0\sigma(z)](1+z^2)\right)\right]} \tag{24}$$

with the dynamical scaling function

$$\sigma(z) = \Omega_K(z)/(1 + z^2) \tag{25}$$

and

$$y_0 = \frac{k_B T\rho}{6\pi\eta\xi\tilde{\alpha}_b} \left(\frac{\partial x}{\partial \mu}\right)_{P,T} \tag{26}$$

Because of the nontrivial dependence of the dynamical scaling function $\sigma(z)$ on $\vec{k}$, the integral in Eq. (24) can be evaluated rigorously only numerically. However, as shown by Kiselev and Kulikov [15], a reasonable approximation for this integral can be obtained even if we ignore the k dependence of the dynamical function $\sigma(z)$ in Eq. (24) and consider it only at the constant value of the wave number $k = k_D = 0.1q_D$. Integration of Eq. (24) in this case yields

$$\Omega_x(q_D\xi) = \frac{2}{\pi}\left[\arctan(q_D\xi) - \frac{1}{\sqrt{1 + y_D q_D \xi}} \arctan \frac{q_D\xi}{\sqrt{1 + y_D q_D \xi}}\right] \tag{27}$$

with

$$y_D = \frac{6\pi\eta^2}{k_B T \rho q_D (\sigma_0 + y_0^{-1})} \tag{28}$$

where $\sigma_0 = \sigma(k_D \xi)$ with $k_D = 0.1 q_D$.

In order to obtain the crossover equations for the kinetic coefficients $\Delta\tilde{\beta}$ and $\Delta\tilde{\gamma}$ similar to the kinetic coefficient $\Delta\tilde{\alpha}$, we need to know the time-dependent correlation functions $\langle \delta x\, \delta S \rangle$ and $\langle \delta S\, \delta S \rangle$. In the Gaussian approximation the local entropy can be represented in the form [1, 2]

$$S(\vec{r}, t) = -\frac{a}{2T_c} \varphi^2(\vec{r}, t) + \left(\frac{\partial \mu}{\partial T}\right)_{P,x} \varphi(\vec{r}, t) \tag{29}$$

where the coefficient a, critical temperature T_c, and derivative $(\partial\mu/\partial T)_{P,x}$ are functions of P. This definition of the local entropy corresponds exactly to the scalar extra field $q(\vec{r})$ introduced by Siggia et al. in their renormalization-group treatment [33]. With account of Eq. (29), the corresponding expressions for the correlation functions read

$$\langle \delta x(0,0)\, \delta S(\vec{r}, t) \rangle = \left(\frac{\partial \mu}{\partial T}\right)_{P,x} \langle \delta\varphi(0,0)\, \delta\varphi(\vec{r}, t) \rangle \tag{30}$$

$$\langle \delta S(0,0)\, \delta S(\vec{r}, t) \rangle = \left(\frac{\partial \mu}{\partial T}\right)^2_{P,x} \langle \delta\varphi(0,0)\, \delta\varphi(\vec{r}, t) \rangle + \frac{a^2}{4T_c^2} \langle \delta\varphi^2(0,0)\, \delta\varphi^2(\vec{r}, t) \rangle \tag{31}$$

Substitution of Eq. (30) into Eq. (10) yields

$$\Delta\tilde{\beta} = \frac{k_B T \rho}{6\pi\eta\xi} \left(\frac{\partial x}{\partial T}\right)_{P,\mu} \Omega_\beta(q_D \xi) \tag{32}$$

where the crossover function Ω_β coincides with the crossover function for $\Delta\tilde{\alpha}$

$$\Omega_\beta(q_D \xi) = \Omega_\alpha(q_D \xi) \tag{33}$$

Equation (11) for $\Delta\tilde{\gamma}$, with account of Eq. (31), takes the form

$$\Delta\tilde{\gamma} = \frac{k_B T^2 \rho}{6\pi\eta\xi} \left(\frac{\partial \mu}{\partial T}\right)^2_{P,x} \left(\frac{\partial x}{\partial \mu}\right)_{P,T} \Omega_\gamma(q_D \xi) + \frac{k_B T \rho C_{P,x}}{6\pi\eta\xi} \Omega_{1\gamma}(q_D \xi) \tag{34}$$

where $\Omega_\gamma(q_D\xi) \sim \langle \delta\varphi\, \delta\varphi \rangle$ and, as in the previous case, coincides with the crossover function for $\Delta\tilde{\alpha}$,

$$\Omega_\gamma(q_D\xi) = \Omega_\alpha(q_D\xi) \tag{35}$$

The crossover function $\Omega_{1\gamma}(q_D\xi) \sim \langle \delta\varphi^2\, \delta\varphi^2 \rangle$ and a direct integration of Eq. (11) yield a slight logarithmic divergence, $\Omega_{1\gamma} \sim \ln(q_D\xi)$. This nonphysical divergence is a consequence of the Gaussian approximation adopted in this paper. The static correlation function $\langle \delta\varphi^2\, \delta\varphi^2 \rangle$ is proportional to the isobaric specific heat capacity

$$C_{P,x} \sim \int \langle \delta\varphi^2(0)\, \delta\varphi^2(\vec{r}) \rangle\, d\vec{r} \tag{36}$$

which diverges weakly as $\tau^{-\alpha}$ at a consolute critical point, whereas in the Gaussian approximation the critical exponent $\alpha = 0$. Thus within the Gaussian approximation we cannot obtain the correct result for the crossover function $\Omega_{1\gamma}$ from Eqs. (11) and (31) directly. However, in the limit $x \to 0$ the derivative $(\partial x/\partial\mu)_{P,T} \sim x \to 0$, the specific heat capacity $C_{P,x}$ of a binary mixture is transformed to the isobaric specific heat capacity C_P of the pure components, and as one can see from Eq. (34), the kinetic coefficient $\tilde{\gamma}$ tends to the thermal conductivity λ of the one-component fluids ($\tilde{\gamma} \to \lambda$).[3] Thus in the limit of pure components the crossover function $\Omega_{1\gamma}(q_D\xi)$ has to transform to the crossover function of one-component fluids $\Omega(q_D\xi)$. It means that the actual form of the crossover function $\Omega_{1\gamma}(q_D\xi)$ can be derived from the mode-coupling equation for the thermal diffusivity of one-component fluids. The mode-coupling theory of critical dynamics yields the following integral for the singular contribution to the thermal diffusivity $D_T = \lambda/\rho C_P$ [30–32]:

$$\Delta D_T(q) = \frac{\Delta\lambda(q)}{\rho C_P(q)}$$

$$= \frac{k_B T}{(2\pi)^3 \rho} \int_0^{q_D} d\vec{k} \left[\frac{C_P(|\vec{q}-\vec{k}|)}{C_P(q)} \right] \frac{\sin^2\Theta}{k^2\eta(k)/\rho + |\vec{q}-\vec{k}|^2\, D_T(|\vec{q}-\vec{k}|)} \tag{37}$$

where $\Delta\lambda = \lambda - \lambda_b$ is the singular part of the thermal conductivity λ, λ_b the regular or background part, and $\vec{q}$ the wave vector of the fluctuations,

[3] The crossover of the thermal conductivity of a binary mixture in the limit of pure components is discussed in more detail in Refs. 6, 7, and 15.

while Θ is the polar angle of $\vec{k}$ with respect to $\vec{q}$. In the hydrodynamic limit ($q \to 0$) and under the following assumptions,

$$C_P(k) = \frac{C_P(0)}{1 + (k\xi)^2}, \qquad \eta(k) = \eta(0), \qquad D_T(k) = [\Delta\lambda(0)\,\sigma(k_D\xi) + \lambda_b]/\rho C_P(k) \tag{38}$$

we obtain after integration

$$\Omega(q_D\xi) = \Omega_{1,2}(q_D\xi)$$
$$= \frac{2}{\pi}\left[\arctan(q_D\xi) - \frac{1}{\sqrt{1 + y_{1D}q_D\xi}} \arctan \frac{q_D\xi}{\sqrt{1 + y_{1D}q_D\xi}}\right] \tag{39}$$

with

$$y_{1D} = \frac{6\pi\eta^2}{k_B T \rho q_D(\sigma_0 + y_1^{-1})} \tag{40}$$

where $y_1 = k_B T \rho C_{P,\mu}/6\pi\eta\xi\tilde{\gamma}_b$ with $C_{P,\mu} = T(\partial S/\partial T)_{P,\mu}$, and $\sigma_0 = \sigma(k_D\xi)$. In the case $y_{1D} = y_D$ the crossover function $\Omega(q_D\xi)$ coincides again with the crossover function $\Omega_x(q_D\xi)$.

As one can see from Eqs. (27) and (39) the crossover functions Ω_x and Ω contain the correlation length as an argument. This means that the crossover behavior of the transport coefficients of a binary mixture depends strongly on the definition of the correlation length. Equations (27) and (39) have been obtained in the Ornstein–Zernike approximation for the correlation function. In this approximation we took into account only the first term $\propto k^2$ in an expansion of the effective Hamiltonian of the system in powers of the wave vector $\vec{k}$. Near the critical point the main contribution to the integral arises from components with small values of the wave number; therefore, this approximation is substantiated. However, as we are interested in the crossover behavior of the kinetic coefficients, the next terms in the effective Hamiltonian have to be considered. In order to take into account a difference of the static correlation function of the order parameter in the crossover region from its Ornstein–Zernike approximation, let us consider the effective Hamiltonian in the form

$$H = \tfrac{1}{2}\int (a\tau\varphi^2 + c(\nabla\varphi)^2 + c_1^2(\Delta\varphi)^2)\, d\vec{r} = \tfrac{1}{2}\sum_{\vec{k}} (a\tau + ck^2 + c_1^2 k^4)\, |\varphi_{\vec{k}}|^2 \tag{41}$$

The details of the calculations of the crossover function in this case are presented in the Appendix. The main result of these calculations is that we

can simply replace the Ornstein–Zernike correlation length in Eqs. (27) and (39) by the renormalized correlation length.

Finally, the crossover expressions for the kinetic coefficients of a binary mixture can be written in the form

$$\tilde{\alpha} = \frac{k_B T \rho}{6\pi\eta\hat{\xi}} \left(\frac{\partial x}{\partial \mu}\right)_{P,T} \Omega_x(q_D\hat{\xi}) + \tilde{\alpha}_b \tag{42}$$

$$\tilde{\beta} = \frac{k_B T \rho}{6\pi\eta\hat{\xi}} \left(\frac{\partial x}{\partial T}\right)_{P,\mu} \Omega_x(q_D\hat{\xi}) + \tilde{\beta}_b \tag{43}$$

$$\tilde{\gamma} = \frac{k_B T^2 \rho}{6\pi\eta\hat{\xi}} \left(\frac{\partial x}{\partial \mu}\right)_{P,T} \left(\frac{\partial \mu}{\partial T}\right)^2_{P,x} \Omega_x(q_D\hat{\xi}) + \frac{k_B T \rho C_{P,x}}{6\pi\eta\hat{\xi}} \Omega(q_D\hat{\xi}) + \tilde{\gamma}_b \tag{44}$$

where the crossover functions $\Omega_x(q_D\hat{\xi})$ and $\Omega(q_D\hat{\xi})$ are given by Eqs. (27) and (39) but with the renormalized correlation length

$$\hat{\xi} = \xi_{OZ}\left[1 - \left(\frac{l_0}{\xi_{OZ}}\right)^2\right] \tag{45}$$

Here

$$\xi_{OZ} = \xi_0 \sqrt{\frac{\tilde{\chi}}{\Gamma_0}} \tag{46}$$

corresponds to the Ornstein–Zernike approximation for the correlation length, ξ_0 and Γ_0 are the amplitudes of the asymptotic power laws for the correlation length and reduced isomorphic compressibility $\tilde{\chi} = \rho(\partial\rho/\partial P)_{T,\mu} P_c \rho_c^{-2}$, respectively, and l_0 is a characteristic length, which is of the order of an average distance between particles. Asymptotically close to the critical point $q_D\hat{\xi} \gg 1$, the singular parts of the kinetic coefficients are much larger than the regular (background) parts ($y_0 \gg 1$, $y_1 \gg 1$, $y_D \approx y_{1D} \approx 1$), all crossover functions approach unity, and Eqs. (42)–(44) in the critical limit reduce to the asymptotic solution given by Eqs. (3)–(5). Far away from the critical point, i.e., $q_D\hat{\xi} \ll 1$, the crossover functions tend to zero ($\Omega_x \to \Omega \to 0$), and all kinetic coefficients approach their regular parts.

3. THERMAL CONDUCTIVITY AND THERMODIFFUSION RATIO

The thermal conductivity of the mixture λ is defined by the equations [28]

$$\vec{J}_d = 0, \qquad \vec{J}_q = -\lambda \nabla T \tag{47}$$

which, according to Eqs. (42)–(44), lead to the following expression for thermal conductivity of binary mixtures [15]:

$$\lambda = \tilde{\gamma} - T\frac{\tilde{\beta}^2}{\tilde{\alpha}} = \frac{k_B T \rho C_{P,x}}{6\pi\eta\hat{\xi}}\,\Omega(q_D\hat{\xi}) + \tilde{\alpha}_b \mu_T^2 T Q(y) + \tilde{\gamma}_b \tag{48}$$

where the crossover function $\Omega_x(q_D\hat{\xi})$ appears only in the argument

$$y = \Delta\tilde{\alpha}/\tilde{\alpha}_b = y_0\Omega_x(q_D\hat{\xi}) = \frac{k_B T\rho}{6\pi\eta\hat{\xi}\tilde{\alpha}_b}\,\mu_x^{-1}\Omega_x(q_D\hat{\xi}) \tag{49}$$

of the new crossover function

$$Q(y) = \frac{y(1+2y^*) - (y^*)^2}{1+y} \tag{50}$$

Here we have introduced the notations $\mu_x = (\partial\mu/\partial x)_{P,T}$, $\mu_T = (\partial\mu/\partial T)_{P,x}$, and $y^* = \tilde{\beta}_b/\mu_T\tilde{\alpha}_b$. Thus the crossover behavior of the thermal conductivity of a binary mixture in the critical region is determined by the function $Q(y)$. Far away from the critical point, where the singular part of the kinetic coefficient $\Delta\tilde{\alpha}$ is negligibly small compared with the regular part $\tilde{\alpha}_b$, or $y \ll 1$ ($q_D\hat{\xi} \ll 1$, $\Omega \simeq \Omega_x \ll 1$), the function $Q(y) \cong -(y^*)^2 + (1+y^*)^2\, y$, and the thermal conductivity reads

$$\lambda \cong \frac{k_B T\rho}{6\pi\eta\hat{\xi}}\left[C_{P,\mu} - \frac{T\tilde{\beta}_b}{\tilde{\alpha}_b}(2+y^*)\,\mu_T\mu_x^{-1}\right]\Omega(q_D\hat{\xi}) + \lambda_b \tag{51}$$

where $C_{P,\mu} = C_{P,x} + T\mu_T^2\mu_x^{-1}$, and the regular (background) part

$$\lambda_b = \tilde{\gamma}_b - \tilde{\alpha}_b T\mu_T^2 (y^*)^2 = \tilde{\gamma}_b - T\frac{\tilde{\beta}_b^2}{\tilde{\alpha}_b} \tag{52}$$

Asymptotically close to the critical point, where the singular part $\Delta\tilde{\alpha}$ is much larger than the regular part $\tilde{\alpha}_b$, the parameter $y \gg 1$ ($q_D\hat{\xi} \gg 1$, $\Omega \cong \Omega_x \cong 1$), function $Q(y) \cong 1 + 2y^* - (1+y^*)^2/y$, and the thermal conductivity tends to its critical background value as

$$\lambda \cong \frac{k_B T\rho}{6\pi\eta\hat{\xi}}\,C_{P,x} - \tilde{\alpha}_b(1+y^*)^2\,T\frac{\mu_T^2}{y} + \lambda_{cb} \tag{53}$$

At the critical point of binary mixtures the first two terms on the right-hand side of Eq. (53) are equal to zero ($C_{P,x}/\hat{\xi} \propto \tau^{-\alpha+\nu} \to 0$, $y^{-1} \propto \mu_x \hat{\xi} \propto \tau^{\gamma-\nu} \to 0$), and the thermal conductivity remains finite,

$$\lim_{\tau(x)\to 0} \lambda = \lambda_{cb} \tag{54}$$

where the critical background

$$\lambda_{cb} = \lambda_b + T\mu_T^2 \tilde{\alpha}_b (1 + y^*)^2 \tag{55}$$

is not equal to the regular part λ_b.

In order to analyze the temperature dependence of the thermal conductivity of a binary mixture, let us consider the critical isochore. At the critical isochore $\rho = \rho_c(x)$ in the temperature region $\tau(x) \ll 1$, where the asymptotic power laws $\hat{\xi} \simeq \xi_0 \tau^{-\nu}$ and $k_B T \mu_x^{-1} \simeq \Gamma_{0\mu} \tau^{-\gamma}$ are valid, the condition $y = 1$ determines a characteristic temperature

$$\tau_D \simeq \left(\frac{\rho_c \Gamma_{0\mu}}{6\pi\eta\xi_0 \tilde{\alpha}_b} \right)^{1/\gamma-\nu} \tag{56}$$

The temperature τ_D is equivalent to the characteristic temperature t_D introduced by Onuki [6]. In the temperature range $\tau_D \ll \tau \ll 1$ the specific heat capacity $C_{P,\mu} \propto \mu_x^{-1} \propto \tau^{-\gamma}$, the parameter $y \ll 1$, and the thermal conductivity of a binary mixture exhibits one-component-like behavior,

$$\lambda - \lambda_b \simeq \text{Const}\, \tau^{-\gamma+\nu} \tag{57}$$

At temperatures $\tau \ll \tau_D$, the parameter $y \gg 1$, and according to Eqs. (53) and (55), the singular part of the thermal conductivity of a binary mixture tends to a finite value at the critical point,

$$\lambda - \lambda_b \simeq T\mu_T^2 \tilde{\alpha}_b (1 + y^*)^2 - \text{Const}\, \tau^{\gamma-\nu} \tag{58}$$

In order to calculate the thermo- and barodiffusivity it is useful to represent the diffusion current in the following form [28]:

$$\vec{J}_d = -\rho D \nabla x - \frac{\rho D_T}{T} \nabla T - \frac{\rho D_P}{P} \nabla P \tag{59}$$

where the binary diffusion coefficient

$$D = \frac{\tilde{\alpha}}{\rho} \mu_x \tag{60}$$

the thermal-diffusion coefficient

$$D_T = \frac{T}{\rho}(\tilde{\alpha}\mu_T + \tilde{\beta}) \tag{61}$$

and barodiffusivity

$$D_P = \frac{\tilde{\alpha}P}{\rho}\left(\frac{\partial \mu}{\partial P}\right)_{T,x} \tag{62}$$

The thermodiffusion ratio with account of Eqs. (42), (43), and (61) can be represented in the form

$$k_T = \frac{D_T}{D} = T\mu_T \mu_x^{-1} K(y) \tag{63}$$

with

$$K(y) = \frac{1 + y^*}{1 + y} \tag{64}$$

In the critical region, where $y \gg 1$ ($\tau \ll \tau_D$), μ_T remains constant, and the thermal-diffusion ratio at the critical isochore diverges as the correlation length,

$$k_T \cong \frac{6\pi\tilde{\alpha}_b}{k_B \rho}\mu_T(1 + y^*)\,\hat{\xi} \sim \tau^{-\nu} \tag{65}$$

and as μ_x^{-1} when $y \ll 1$ ($\tau \gg \tau_D$),

$$k_T \cong T\mu_T \mu_x^{-1}(1 + y^*) \sim \tau^{-\gamma} \tag{66}$$

These predictions for the temperature dependencies of the thermal conductivity and the thermal-diffusion ratio at the critical isochore of a binary mixture are consistent with Onuki's predictions [6] and are restricted to the region $\tau(x) \ll 1$, where the asymptotic scaling laws for all thermodynamic quantities are valid. For fluids and fluid mixtures this region is restricted by the temperatures $\tau \leqslant 10^{-3}$ [34, 35]; therefore, for the numerical analysis of experimental data the crossover expressions, Eqs. (48) and (63), together with the crossover equation of state for binary mixtures have to be used.

4. CROSSOVER FREE ENERGY FOR CARBON DIOXIDE AND ETHANE MIXTURES

In the present paper we used the crossover model for the isomorphic free energy of binary mixtures recently obtained by Kiselev [26]. The isomorphic free-energy density of a binary mixture is given by

$$\rho\tilde{A}(T, \rho, \tilde{x}) = \rho A(T, \rho, x) - \rho\mu x(T, \rho, \tilde{x}) \tag{67}$$

where $\rho A(T, \rho, x)$ is the Helmholtz free-energy density of the mixture, and the isomorphic variable $\tilde{x}$ is related to the field variable ζ, first introduced by Leung and Griffiths [36], by the relation

$$\tilde{x} = 1 - \zeta = \frac{e^{\mu/RT}}{1 + e^{\mu/RT}} \tag{68}$$

The thermodynamic equation

$$x = -\tilde{x}(1 - \tilde{x}) \left(\frac{\partial \tilde{A}}{\partial \tilde{x}}\right)_{T, \rho} \frac{1}{RT} \tag{69}$$

(where R is the universal gas constant) provides a relation between the concentration x and the isomorphic variable $\tilde{x}$. At fixed $\tilde{x}$ the isomorphic free energy $\rho\tilde{A}$ is the same function of τ and ρ as the Helmholtz free-energy density of a one-component fluid,

$$\begin{aligned} \frac{\rho\tilde{A}(T, \rho, \tilde{x})}{R\rho_{c0}T_{c0}} = {} & \tilde{k}r^{2-\alpha}R^{\alpha}(q)\left[\tilde{a}\Psi_0(\theta) + \sum_{i=1}^{4} \tilde{c}_i r^{\Delta_i} R^{-\tilde{\Delta}_i}(q)\, \Psi_i(\theta)\right] \\ & + \sum_{i=1}^{4} \left(\tilde{A}_i + \frac{\rho}{\rho_{c0}}\tilde{m}_i\right) \tau^i(\tilde{x}) - \frac{P_c(\tilde{x})}{R\rho_{c0}T_{c0}} \\ & + \frac{\rho T}{\rho_{c0}T_{c0}} [\ln(1 - \tilde{x}) + \tilde{m}_0] \end{aligned} \tag{70}$$

$$\tau = \frac{T - T_c(\tilde{x})}{T_c(\tilde{x})} = r(1 - b^2\theta^2) \tag{71}$$

$$\Delta\rho = \frac{\rho - \rho_c(\tilde{x})}{\rho_c(\tilde{x})} = \tilde{k}r^{\beta}R^{-\beta+1/2}(q)\,\theta + \tilde{d}_1\tau \tag{72}$$

where α, β, and Δ_i are universal critical exponents, and b^2 is the universal linear-model parameter. The values of these universal constants are listed in Table I. The universal scaled functions $\Psi_i(\theta)$ and the crossover function

Table I. Universal Constants in the Helmholtz Free-Energy Density

$\alpha = 0.110$
$\beta = 0.325$
$\gamma = 2 - \alpha - 2\beta = 1.24$
$b^2 = (\gamma - 2\beta)/\gamma(1 - 2\beta) = 1.359$
$\Delta_1 = \tilde{\Delta}_1 = 0.51$
$\Delta_2 = \tilde{\Delta}_2 = 2\Delta_1 = 1.02$
$\Delta_3 = \Delta_4 = \gamma + \beta - 1 = 0.565$
$\tilde{\Delta}_3 = \tilde{\Delta}_4 = \Delta_3 - \frac{1}{2} = 0.065$

$R(q)$ are the same as those in the parametric crossover model employed earlier by Kiselev [26],

$$\Psi_i(\theta) = \sum_{j=0}^{5} \alpha_{ij}\theta^j \qquad (i = 0,..., 4) \tag{73}$$

where α_{ij} are universal constants, and

$$R(q) = \left(1 + \frac{q^2}{1+q}\right)^2 \tag{74}$$

where the variable q is related to the parametric variable r by

$$q = (rg)^{1/2} \tag{75}$$

As demonstrated in a previous publication [9], the system-dependent coefficient g is proportional to the inverse Ginzburg number Gi.

All system-dependent parameters in Eqs. (70)–(72) as well as the critical parameters $T_c(\tilde{x})$, $\rho_c(\tilde{x})$, and $P_c(\tilde{x})$ are analytic functions of the isomorphic variable $\tilde{x}$. For the critical parameters we use the same expressions as in our previous papers [26, 37],

$$T_c(\tilde{x}) = T_{c0}(1-\tilde{x}) + T_{c1}\tilde{x} + \tilde{x}(1-\tilde{x}) \sum_{i=0}^{2} T_i(1-2\tilde{x})^i \tag{76}$$

$$\rho_c(\tilde{x}) = \rho_{c0}(1-\tilde{x}) + \rho_{c1}\tilde{x} + \tilde{x}(1-\tilde{x}) \sum_{i=0}^{2} \rho_i(1-2\tilde{x})^i \tag{77}$$

$$P_c(\tilde{x}) = P_{c0}(1-\tilde{x}) + P_{c1}\tilde{x} + \tilde{x}(1-\tilde{x}) \sum_{i=0}^{2} P_i(1-2\tilde{x})^i \tag{78}$$

where the subscripts 0 and 1 correspond to the first and second components of the mixture, respectively.

In addition to Eqs. (76)–(78), we also adopted a so-called critical line condition which implies that a zero level of the chemical potential of a binary mixture can be chosen so that the isomorphic variable $\tilde{x} = x$ along the whole critical line, including the one-component limits. For the thermodynamic potential as given by Eqs. (70)–(72), the critical-line condition can be written in the form

$$\frac{d\tilde{m}_0}{d\tilde{x}} = \frac{1}{R\rho_c T_c}\frac{dP_c}{d\tilde{x}} + \left(\frac{\rho_{c0}}{\rho_c}\tilde{A}_1 + \tilde{m}_1\right)\frac{T_{c0}}{T_c^2}\frac{dT_c}{d\tilde{x}} \tag{79}$$

In this case, along the whole critical line $\tilde{x} = x$, and

$$T_c(\tilde{x}) = T_c(x), \qquad \rho_c(\tilde{x}) = \rho_c(x), \qquad P_c(\tilde{x}) = P_c(x) \tag{80}$$

To specify the crossover equation for $\tilde{A}(T, \rho, \tilde{x})$ of a binary mixture, we also need the system-dependent parameters $\tilde{d}_1(\tilde{x})$, $\tilde{k}(\tilde{x})$, $\tilde{a}(\tilde{x})$, $\tilde{c}_i(\tilde{x})$, $\tilde{g}(\tilde{x})$, $\tilde{m}_i(\tilde{x})$, and $\tilde{A}_i(\tilde{x})$ as functions of the isomorphic variable $\tilde{x}$. To represent all these system-dependent parameters in Eqs. (70)–(72), designated $\tilde{k}_i(\tilde{x})$, as functions of $\tilde{x}$ we used an isomorphic generalization of the law of corresponding states [26, 37], which, for $\tilde{k}$ and $\tilde{d}_1$, written in the form

$$\tilde{k}_i(\tilde{x}) = k_{i0} + (k_{i1} - k_{i0})\,\tilde{x} + k_i^{(1)}\,\Delta Z_c(\tilde{x}) \tag{81}$$

and, for all others coefficients, reads

$$\tilde{k}_i(\tilde{x}) = \frac{P_c(\tilde{x})}{R\rho_{c0}T_{c0}}\left[k_{i0} + (k_{i1} - k_{i0})\,\tilde{x} + k_i^{(1)}\,\Delta Z_c(\tilde{x})\right] \tag{82}$$

In Eqs. (81) and (82) $k_i^{(1)}$ are mixing coefficients, and

$$\Delta Z_c(\tilde{x}) = Z_c(\tilde{x}) - Z_{cid}(\tilde{x}) \tag{83}$$

is a difference between the actual compressibility factor of a mixture $Z_c(\tilde{x}) = P_c(\tilde{x})/R\rho_c(\tilde{x})\,T_c(\tilde{x})$ and its ideal part $Z_{cid}(\tilde{x}) = Z_{c0}(1-\tilde{x}) + Z_{c1}\tilde{x}$.

In the present work the coefficients T_i, ρ_i, and P_i in Eqs. (76)–(78) and the mixing coefficients $k_i^{(1)}$ were determined from a fit of Eqs. (70)–(72) to experimental thermodynamic-property data for carbon dioxide and ethane mixtures in the one-phase region.

For pure ethane we adopted the same parameters as obtained by Kiselev [26], while for pure carbon dioxide all system-dependent parameters have been found from a fit of Eqs. (70)–(74) to the experimental P, ρ, T data obtained by Wagner and co-workers [38, 39], by Michels and Michels [40], by Holste et al. [41], and by Fenghour et al. [42]. The coefficients $\tilde{m}_i$, which determine the temperature behavior of the

Table II. System-Dependent Constants for Mixtures of Carbon Dioxide and Ethane

	k_i, CO_2	k_i, C_2H_6	$k_i^{(1)}$, mixtures
	Critical amplitudes		
k	1.2245	1.2015	2.9683
d_1	−0.9221	0.2977	−145.07
a	22.0281	17.779	−161.25
c_1	−6.0906	2.9728	4902.1
c_2	6.6229	12.776	0
c_3	−11.773	−18.125	−3972.8
c_4	12.122	1.1248	4900.6
	Crossover parameter		
g	0.1477	1.3869	1100.5
	Background coefficients		
A_1	−7.0198	−6.4155	16.762
A_2	19.138	20.847	−1532.5
A_3	1.8125	3.2112	0
m_1	0	0	−0.62963
$\Delta m_1 = m_{11} - m_{10}$			8.5218
m_2	−10.094	−18.136	1343.5
m_3	3.1208	−0.1729	1209.2
m_4	0.5476	0.1176	0
	Molar mass		
$g \cdot mol^{-1}$	44.01	30.069	

specific heat capacity at the critical isochore, were found from a fit to the experimental C_v data obtained by Magee and Ely [43]. The values of all system-dependent constant for pure carbon dioxide and ethane are listed in Table II. A comparison with the experimental data is shown in Figs. 1 and 2. Good agreement between experimental and calculated values of the pressure and the specific heat capacity is observed in the range of temperatures and densities bounded by

$$0.995T_c \leqslant T \leqslant 1.4T_c, \qquad 0.35\rho_c \leqslant \rho \leqslant 1.65\rho_c \tag{84}$$

To determine the system-dependent parameters in the crossover equation for carbon dioxide and ethane mixtures, we used the following experimental information:

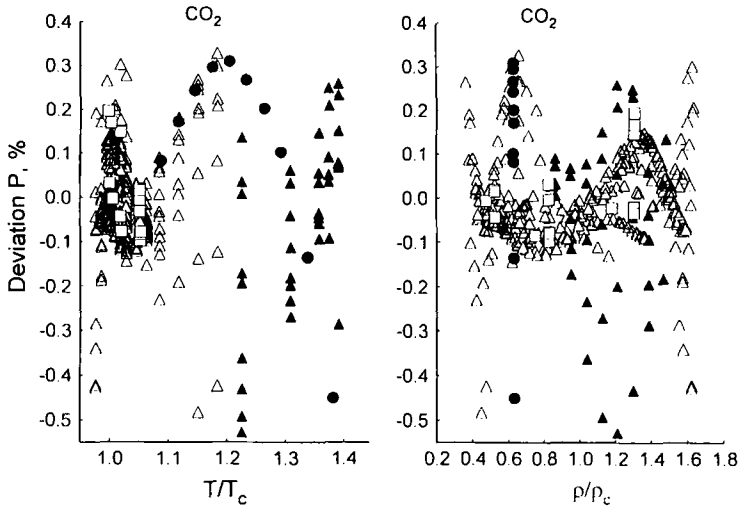

Fig. 1. Percentage deviations of the experimental pressures obtained by Wagner and co-workers [38, 39] (open triangles), by Michels and Michels [40] (filled triangles), by Holste et al. [41] (open squares), and by Fenghour and co-workers [42] (filled circles) from values calculated with the crossover equation of state.

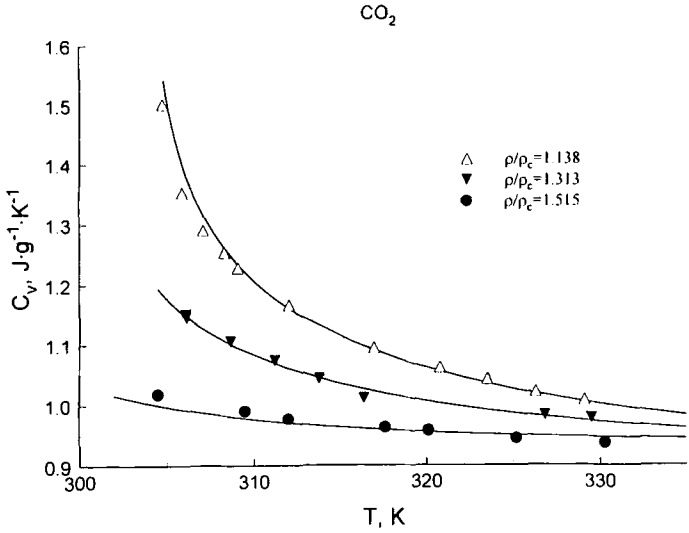

Fig. 2. The isochoric specific heat capacity C_v of carbon dioxide at densities $\rho = 1.138\rho_c$, $\rho = 1.313\rho_c$, and $\rho = 1.515\rho_c$ as a function of temperature. The symbols indicate the experimental data obtained by Magee and Ely [43] and the curves represent values calculated with the crossover model.

(i) experimental P–ρ–T–x data obtained by Weber [44] for three concentrations (0.26022, 0.50755, and 0.74834 mol fractions of ethane);

(ii) experimental P–ρ–T–x data obtained by Lau [25] for four concentrations (0.09633, 0.26022, 0.50755, and 0.74834 mol fractions of ethane); and

(iii) experimental specific heat capacities obtained by Magee [24] for three concentrations (0.26022, 0.50755, and 0.74834 mol fractions of ethane).

The values of the coefficients T_i, ρ_i, and P_i in Eqs. (76)–(78) for the critical parameters, as well as the mixing coefficients $k_i^{(1)}$ in the crossover equation of state, were determined from a fit to all sets of experimental P–ρ–T–x and specific heat capacities data simultaneously. As for pure fluids, we used the experimental data in the one-phase region only at temperatures $T \geqslant 0.995 T_c(x)$. The values of the coefficients $k_i^{(1)}$ are presented in Table II, and the values of the coefficients T_i, ρ_i, and P_i for the critical parameters are listed in Table III.

A comparison of the experimental P–ρ–T–x and $C_{v,x}$ data with the results of the calculations is shown in Figs. 3 and 4. One can see that in the range of temperatures $0.995 T_c(x) \leqslant T \leqslant 125 T_c(x)$ and densities $0.4\rho_c(x) \leqslant \rho \leqslant 1.6\rho_c(x)$, the crossover equation gives a good representation of the experimental P–ρ–T–x and $C_{v,x}$ data.

Table III. Critical-Line Parameters for Mixtures of Carbon Dioxide and Ethane

Critical temperature (K)	Critical density (mol · L^{-1})	Critical pressure (MPa)
	Pure CO_2	
$T_{c0} = 304.136$	$\rho_{c0} = 10.625$	$P_{c0} = 7.3773$
	$CO_2 + C_2H_6$	
$T_0 = -54.441$	$\rho_0 = -1.4657$	$P_0 = 7.3773$
$T_1 = -15.715$	$\rho_1 = -3.9207 \times 10^{-1}$	$P_1 = -1.7142$
$T_2 = 4.4935$	$\rho_2 = -7.0024 \times 10^{-2}$	$P_2 = -1.5064$
$T_3 = 10.870$	$\rho_3 = -2.7615 \times 10^{-1}$	$P_3 = -4.9367 \times 10^{-1}$
$T_4 = -1.4019 \times 10^{-2}$	$\rho_4 = -3.5348 \times 10^{-1}$	$P_4 = 9.9349 \times 10^{-1}$
	Pure C_2H_6	
$T_{c1} = 305.322$	$\rho_{c1} = 6.8701$	$P_{c1} = 4.8718$

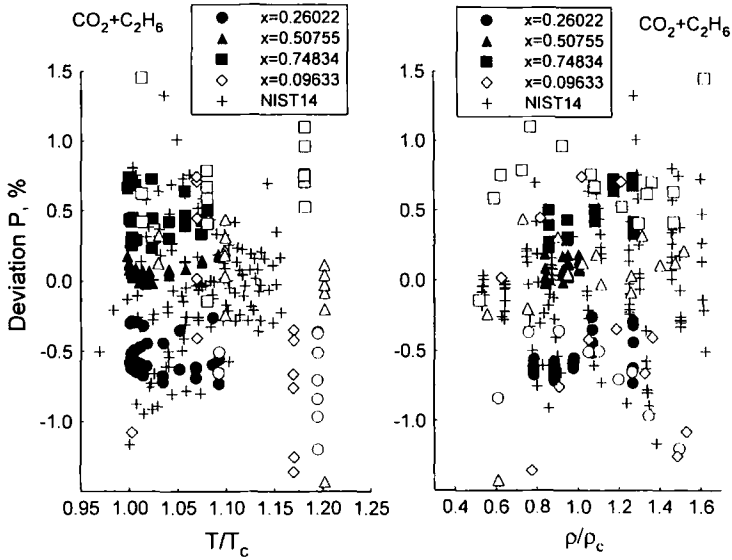

Fig. 3. Percentage deviations of experimental pressures for carbon dioxide and ethane mixtures from values calculated with the crossover equation of state at various concentrations of ethane. The filled symbols indicate the experimental data obtained by Weber [44], the open symbols correspond to the experimental data obtained by Lau [25], and pluses represent the values of densities calculated with the NIST14 program [46] at pressures and temperatures corresponding to the experimental specific heat capacity data of Magee [24].

Even though all adjustable parameters have been found from a fit of Eqs. (70)–(72) to the experimental data in the one-phase region, we can also extrapolate our crossover model to represent the thermodynamic surface of carbon dioxide and ethane mixtures in the two-phase region down to temperatures about 10–15% below the critical temperatures. We applied our crossover model to calculate the thermodynamic properties in the two-phase region near the critical locus. For a comparison of our calculations with experimental data the following experimental information was used:

(i) experimental $P-x$ data of Fredenslund and Mollerup [45],

(ii) experimental $P-x$ data of Ohgaki and Katayama [47],

(iii) experimental $P-x$ data of Brown et al. [48], and

(iv) experimental $P-x$ data of Wei et al. [49].

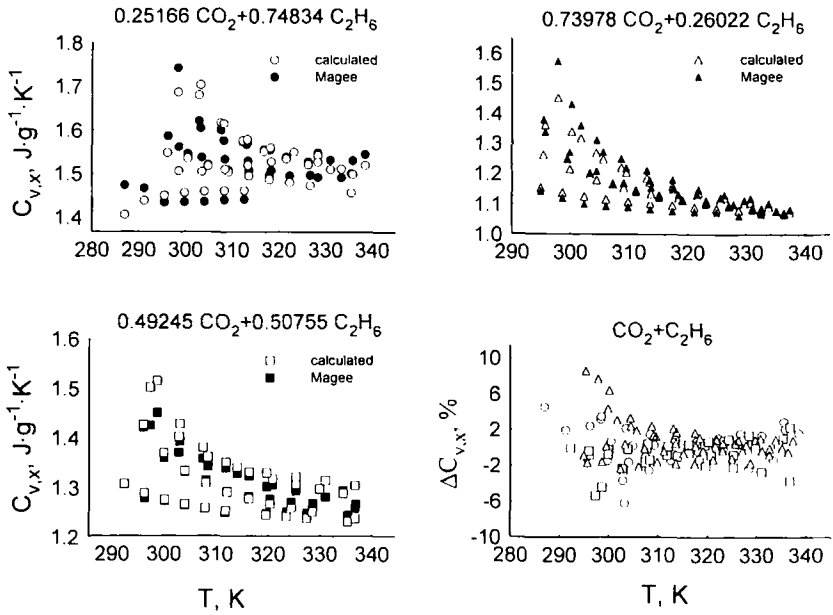

Fig. 4. The isochoric specific heat capacity $C_{v,x}$ of carbon dioxide and ethane mixtures at concentrations $x = 0.74834$, $x = 0.50755$, and $x = 0.26022$ mol fraction of ethane as a function of temperature. The filled symbols indicate the experimental data obtained by Magee [24], and the open symbols represent values calculated with the crossover model.

A comparison between the experimental data and the values calculated from our crossover model is shown in Fig. 5. Good agreement between experimental data and calculated values is observed down to a temperature of 263.15 K. Thus one can see that our new crossover equation of state for carbon dioxide and ethane mixtures is capable of representing the experimental data over a larger range of temperatures and densities than the crossover equation obtained earlier by Jin et al. [22, 23].

5. REGULAR PARTS OF THE TRANSPORT COEFFICIENTS

Equations (48) and (42)–(44) for the transport coefficients in a binary mixture except the thermodynamic derivatives μ_x, μ_T and specific heat capacity $C_{P,x}$ contain also the viscosity and the regular (background) parts of the kinetic coefficients. The viscosity η in these equations represents a high-frequency shear viscosity which is an analytic function of the temperature, the density, and the concentration. In the present work, as in our

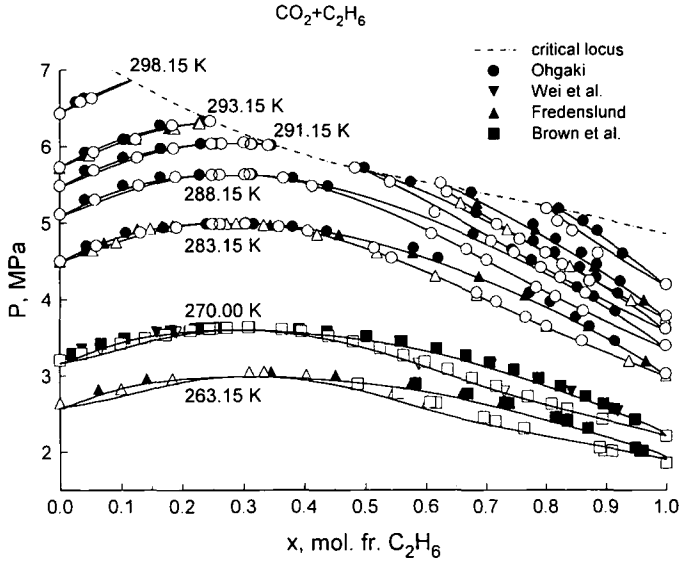

Fig. 5. The pressure–composition diagram for carbon dioxide and ethane mixtures. The symbols indicate experimental data obtained by Fredenslund and Mollerup [45], by Ohgaki and Katayama [47], by Brown et al. [48], and by Wei et al. [49]. The filled symbols indicate saturated liquid data, and the open symbols represent saturated vapor data. The dashed curve represents the critical locus, and the solid curves represent values calculated with the crossover model.

previous papers [15–17], we used for the shear viscosity a corresponding-states correlation in the form

$$\eta(T,\rho,x)=\left[\frac{\eta^{(1)}(T,\rho)[T_c^{(1)}]^{1/6}}{\sqrt{M_1}\,[P_c^{(1)}]^{2/3}}(1-x)+x\frac{\eta^{(2)}(T,\rho)[T_c^{(2)}]^{1/6}}{\sqrt{M_2}\,[P_c^{(2)}]^{2/3}}\right]\sqrt{M_{\mathrm{mix}}}\frac{P_{cx}^{2/3}}{T_{cx}^{1/6}} \tag{85}$$

where M_{mix} is a molecular mass of a mixture, T_{cx} and P_{cx} are to be determined from the Prausnitz and Gunn mixing rules [50, 51]

$$T_{cx}=\sum_{i=1}^{2}x_iT_c^{(i)},\qquad P_{cx}=RT_{cx}\sum_{i=1}^{2}x_iZ_c^{(i)}\Big/\sum_{i=1}^{2}\frac{x_i}{\rho_c^{(i)}} \tag{86}$$

and the critical compressibility factor $Z_c^{(i)}=P_c^{(i)}/R\rho_c^{(i)}T_c^{(i)}$. The superscript $i=1$ corresponds to pure carbon dioxide and $i=2$ to pure ethane,

respectively. The viscosities $\eta^{(1)}$ and $\eta^{(2)}$ of the pure components are written as

$$\eta^{(i)}(T, \rho) = \eta_0^{(i)}(T) + \eta_{\text{exc}}^{(i)}(\rho) \qquad (i = 1, 2) \tag{87}$$

where $\eta_0^{(i)}(T)$ are the viscosities of the pure components in the limit $\rho \to 0$, and $\eta_{\text{exc}}^{(i)}(\rho)$ are the density-dependent excess viscosities [11, 13, 52]

$$\eta_{\text{exc}}^{(i)}(\rho) = \sum_{k=1} \eta_k^{(i)} \left(\frac{\rho}{\rho_c^{(i)}} \right)^k \tag{88}$$

There are no experimental data or any theoretical prediction for the dependencies of the kinetic coefficients $\tilde{\alpha}$ and $\tilde{\beta}$ on the temperature, the density, and the concentration far away from the critical point, where these coefficients tend to their background parts $\tilde{\alpha}_b$ and $\tilde{\beta}_b$, respectively. It is known only that even in the ideal-gas limit the binary diffusion coefficient D and the thermal-diffusion coefficient D_T, related to the kinetic coefficients $\tilde{\alpha}_b$ and $\tilde{\beta}_b$ by Eqs. (60) and (61), are complex functions of the temperature, concentration, and molecular masses [53]. The primary concentration dependence of these coefficients in the ideal-gas limit and in the dilute solutions is given by $\sim x(1-x)$. The background parts of the kinetic coefficients $\tilde{\alpha}$ and $\tilde{\beta}$ can be presented in the form [16, 17]

$$\tilde{\alpha}_b = \tilde{\alpha}_0(T, x) + x(1-x) \sum_{k=1}^{6} \left(\frac{\rho}{\rho_c} \right)^{k+1} [\alpha_{3k} + \alpha_{3k+1}(1-2x) + \alpha_{3k+2}(1-2x)^2] \tag{89}$$

$$\tilde{\beta}_b = \tilde{\beta}_0(T, x) + x(1-x) \sum_{k=1}^{6} \left(\frac{\rho}{\rho_c} \right)^{k+1} [\beta_{3k} + \beta_{3k+1}(1-2x) + \beta_{3k+2}(1-2x)^2] \tag{90}$$

where the ideal-gas parts of the kinetic coefficients are given by

$$\tilde{\alpha}_0 = \frac{\rho D_0 M_{\text{mix}}^2}{RT} x(1-x) \tag{91}$$

$$\tilde{\beta}_0 = R\tilde{\alpha}_0 \left(\beta_1 + x\beta_2 - \ln \frac{x}{1-x} \right) \tag{92}$$

Here α_k and β_k $(k \geqslant 1)$ are system-dependent coefficients, and D_0 is the binary diffusion coefficient in the limit $\rho \to 0$. In practice we used for D_0 an empirical correlation proposed by Fuller et al. [54, 55],

$$D_0 = \frac{10^{-7} T^{1.75} [(M_1 + M_2)/M_1 M_2]^{1/2}}{P[(\sum v)_{CO_2}^{1/3} + (\sum v)_{C_2H_6}^{1/3}]^2} \tag{93}$$

where T is in K, P in atm, and D_0 in $m^2 \cdot s^{-1}$. To determine $\sum v$ the values of the atomic diffusion volumes

$$\left(\sum v\right)_{CO_2} = 26.9, \qquad \left(\sum v\right)_{C_2H_6} = 37.7 \tag{94}$$

were used. The coefficients α_k can be found from fitting the crossover equation (42) together with Eqs. (60) and (89) to the experimental binary diffusion coefficients far away from the critical point. Unfortunately, we do not have these data for carbon dioxide and ethane mixtures. Therefore we generated them with the empirical correlation proposed by Leffler and Gullinan for binary fluid mixtures [56].

$$D\eta = (D_{12}^0 \eta^{(2)})^{x_2} (D_{21}^0 \eta^{(1)})^{x_1} \tag{95}$$

where x_1 and x_2 are the molar fractions of the components, and the dilute-solution binary diffusion coefficients D_{12}^0 and D_{21}^0 were calculated with an empirical modification of the Stokes–Einstein equation for the diffusion coefficient proposed by Lusis and Ratcliff [57],

$$D_{ij}^0 = \frac{8.52 \cdot 10^{-12} T}{\eta^{(j)} V_j^{1/3}} \left[1.40 + \left(\frac{V_j}{V_i}\right)^{2/3} \right] \tag{96}$$

Here T is in K, η in cP, and D_{ij}^0 in $m^2 \cdot s^{-1}$, V_j, and V_i (in $cm^3 \cdot mol^{-1}$) are the molar volumes of components at their normal boiling temperatures. In practice, we used

$$V_{CO_2} = 55.024, \qquad V_{C_2H_6} = 37.321 \tag{97}$$

where for CO_2 the value of the molar volume of liquid carbon dioxide at the triple point was taken. The values found for the coefficients α_k we then used to determine the coefficients β_k. The coefficients β_k in Eq. (90) were found from fitting Eqs. (43) and (63) to the experimental thermal-diffusion ratio data obtained by Walther [58]. The thermodynamic properties for carbon dioxide and ethane mixtures were calculated from the crossover equation of state obtained above. The correlation length $\hat{\xi}$ is given by Eq. (45), where for the bare correlation length ξ_0, the cutoff parameter q_D, and l_0, we used simple linear approximations,

$$\xi_0 = \xi_0^{(1)}(1-x) + \xi_0^{(2)} x \tag{98}$$

$$q_D^{-1} = \frac{1}{q_D^{(1)}}(1-x) + \frac{1}{q_D^{(2)}} x \tag{99}$$

$$l_0 = l_0^{(1)}(1-x) + l_0^{(2)} x \tag{100}$$

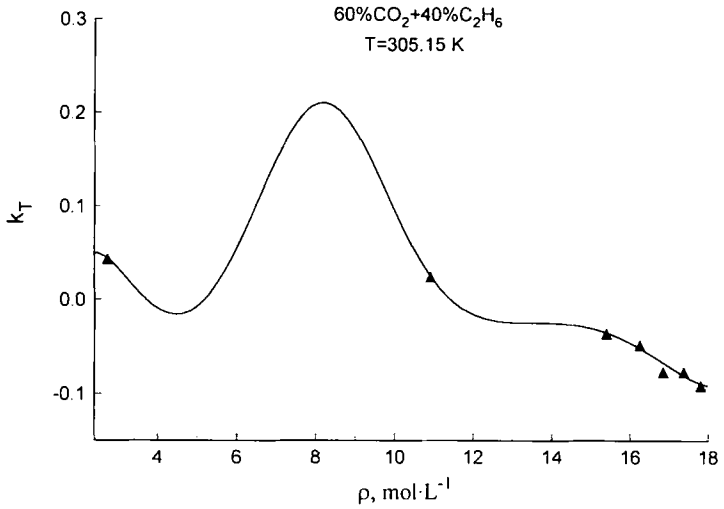

Fig. 6. The thermal diffusion ratio of the carbon dioxide and ethane mixture at temperature $T = 305.15$ K and concentration $x = 0.4$ mol fraction of ethane. The symbols indicate experimental data obtained by Walther [58] and the curve represents values calculated with the crossover model.

The parameter l_0 can be assumed to be the average distance between particles and, in principle, can be considered as an additional adjustable parameter of our model. In the present work, in calculating l_0, for simplicity we set

$$l_0^{(i)} = [q_D^{(i)}]^{-1} = \xi_0^{(i)} \tag{101}$$

where for the system-dependent parameters $\xi_0^{(i)}$, we adopt the values for pure carbon dioxide ($i = 1$) and ethane ($i = 2$) obtained by Olchowy and Sengers [13],

$$\xi_0^{(1)} = 0.15 \text{ nm} \qquad \xi_0^{(2)} = 0.19 \text{ nm} \tag{102}$$

Table IV. Background Thermal Conductivity Coefficients for the Pure Components (λ_k in $W \cdot m^{-1} \cdot K^{-1}$)

Carbon dioxide	Ethane
$\lambda_1^{(1)} = 2.329 \times 10^{-2}$	$\lambda_1^{(2)} = 2.298 \times 10^{-2}$
$\lambda_2^{(1)} = 2.643 \times 10^{-4}$	$\lambda_2^{(2)} = 9.897 \times 10^{-4}$
$\lambda_5^{(1)} = 4.952 \times 10^{-7}$	$\lambda_6^{(2)} = 3.503 \times 10^{-4}$

The coefficients α_k and β_k found in this way are reproduced in Table IV. The values of the coefficients α_k and β_k depend strongly on the equation of state used for the calculation of the thermodynamic derivatives μ_T and μ_x in Eqs. (60) and (63); therefore, they differ from the corresponding values obtained earlier by Kiselev and Povodyrev [16, 17] with the crossover equation of state of Jin et al. [22, 23].

The results of comparison with thermal-diffusion ratio data for the carbon dioxide and ethane mixture is shown in Fig. 6. Good agreement between calculated values and experimental data of Walther [58] for the thermal diffusion ratio is observed. As one can see from Fig. 6, the thermal-diffusion ratio increases in the critical region and reaches the maxima at the density $\rho \simeq 8.32$ mol $\cdot$ L^{-1}, which is close to the critical density at this composition.

6. COMPARISON WITH EXPERIMENTAL THERMAL-CONDUCTIVITY DATA

In order to compare the crossover model with experimental thermal-conductivity data, in addition to the equation of state and expressions for the background transport coefficients $\tilde{\alpha}_b$, $\tilde{\beta}_b$, and η_b, one needs the background part $\tilde{\gamma}_b$ of the kinetic coefficient $\tilde{\gamma}$. This quantity can be written in the form [16, 17]

$$\tilde{\gamma}_b = \tilde{\gamma}_0(T, x) + \Delta\lambda_b^{(1)}(1-x) + \Delta\lambda_b^{(2)}x + x(1-x)\sum_{k=1}^{6}(\gamma_{2k-1} + \gamma_{2k}x)\left(\frac{\rho}{\rho_c}\right)^k \tag{103}$$

where $\tilde{\gamma}_0$ determines the ideal-gas limit of $\tilde{\gamma}_b$, $\Delta\lambda_b^{(1)}$ and $\Delta\lambda_b^{(2)}$ define the nonideal parts of the thermal conductivity λ_b in the limits of the pure components, and the third part determines the nonideal part of the kinetic coefficient $\tilde{\gamma}_b$ in binary mixtures. An expression for $\tilde{\gamma}_0$ in accordance with Eq. (52) reads

$$\tilde{\gamma}_0(T, x) = \lambda_0(T, x) + T\frac{\tilde{\beta}_0^2(T, x)}{\tilde{\alpha}_0(T, x)} \tag{104}$$

where for $\lambda_0(T, x)$ we use a simple expression proposed by Wassilijeva [59],

$$\lambda_0(T, x) = \frac{(1-x)\lambda_0^{(1)}(T)}{(1-x) + xA_{12}} + \frac{x\lambda_0^{(2)}(T)}{x + (1-x)A_{21}} \tag{105}$$

Table V. The Background Kinetic Coefficients (α_k in $kg \cdot s \cdot m^{-3}$, β_1 Dimensionless, β_k in $kg \cdot m^{-1} \cdot s^{-1} \cdot K^{-1}$, γ_k in $W \cdot m^{-1} \cdot K^{-1}$)

Coefficient for $\tilde{\alpha}_b$		Coefficient for $\tilde{\beta}_b$		Coefficient for $\tilde{\gamma}_b$	
α_6	4.6125×10^{-11}	β_1	3.4721	γ_1	-3.7435×10^{-1}
α_7	6.6796×10^{-11}	β_3	-1.0450×10^{-6}	γ_2	4.6099×10^{-1}
α_{12}	-2.5779×10^{-11}	β_6	9.1371×10^{-7}	γ_5	1.2749×10^{-1}
α_{13}	-2.7020×10^{-11}	β_{12}	-1.7185×10^{-7}	γ_9	1.3688×10^{-2}
α_{18}	2.6450×10^{-12}	β_{18}	1.4604×10^{-8}	γ_{10}	-9.5232×10^{-2}
α_{19}	2.5930×10^{-12}				

with the Lindsay and Bromley [60] modification for A_{12} and A_{21}:

$$A_{12} = \frac{1}{4}\left\{1 + \left[\frac{\eta^{(1)}(T,0)}{\eta^{(2)}(T,0)}\left(\frac{M_2}{M_1}\right)^{3/4}\frac{T+S_1}{T+S_2}\right]^{1/2}\right\}^2 \frac{T+S_{12}}{T+S_1}$$
$$A_{21} = \frac{1}{4}\left\{1 + \left[\frac{\eta^{(2)}(T,0)}{\eta^{(1)}(T,0)}\left(\frac{M_1}{M_2}\right)^{3/4}\frac{T+S_2}{T+S_1}\right]^{1/2}\right\}^2 \frac{T+S_{12}}{T+S_2} \tag{106}$$

Here $\lambda_0^{(i)} = (i = 1, 2)$ is the thermal conductivity in the ideal-gas limit, $S_1 = 1.5T_{nb}^{(1)}$, $S_2 = 1.5T_{nb}^{(2)}$ and $S_{12} = \sqrt{S_1 S_2}$ are Sutherlend constants, and

$$T_{nb}^{(1)} = 191.65 \text{ K}, \qquad T_{nb}^{(2)} = 284.52 \text{ K} \tag{107}$$

are the normal boiling temperatures of the pure components.[4] In the limits of the pure components $\tilde{\alpha}_b \equiv \tilde{\beta}_b \equiv 0$ [see Eqs. (89)–(92)], and Eq. (48) for the thermal conductivity in binary mixtures with account of Eq. (103) is transformed into the crossover equation for the thermal conductivity of one-component fluids:

$$\lambda = \frac{k_B T \rho C_P}{6\pi\eta\xi}\Omega(q_D\xi) + \lambda_b^{(i)}(T, \rho) \tag{108}$$

where $\lambda_b^{(i)}(T, \rho)$ is the background part of the thermal conductivity of pure components. As noted earlier by Sengers and co-workers [12, 13, 62], the excess functions $\Delta\lambda_b^{(i)} = \lambda_b^{(i)} - \lambda_0^{(i)}$ can be treated as functions of the density only, so that

$$\lambda_b^{(i)}(T, \rho) = \lambda_0^{(i)}(T) + \sum_k \lambda_k^{(i)}\left(\frac{\rho}{\rho_c^{(i)}}\right)^k \tag{109}$$

[4] For pure CO_2 the value of the triple-point temperature was used.

with

$$\lambda_0^{(i)}(T) = \sqrt{T} \Big/ \sum_j \lambda_{0j}^{(i)} T^{-j} \tag{110}$$

For the coefficients $\lambda_{0j}^{(i)}$ we adopt the same values as used by Olchowy and Sengers [13] for pure carbon dioxide and ethane, but the coefficients $\lambda_k^{(i)}$ have been determined from a fit of the crossover equation (108) to the experimental data for the thermal conductivity of carbon dioxide obtained by Michels et al. [61] and the thermal conductivity of ethane obtained by Mostert et al. [62]. The coefficients $\lambda_k^{(i)}$ for carbon dioxide and ethane are presented in Table IV. The results of fitting the crossover equation (108) to the experimental thermal conductivity data for CO_2 and C_2H_6 are shown in Figs. 7 and 8. Good agreement between the calculated values of the thermal conductivity and the experimental data is observed.

In order to reproduce a global thermal-conductivity surface for the mixtures of carbon dioxide and ethane over the entire range of concentrations we need to know the coefficients γ_k. Since these coefficients determine the concentration and density dependence of the regular part of the thermal conductivity [see Eqs. (52) and (103)], we could in principle find them from fitting the crossover equation to the experimental thermal-conductivity data far away from the critical point. Since we do not have such data for carbon dioxide and ethane mixtures, in the present work the coefficients γ_k in Eq. (103) have been found from a fit of the crossover equation (48) to the experimental thermal-conductivity data for carbon dioxide and ethane mixtures in the critical region obtained by Mostert [63]. The coefficients γ_k are presented in Table IV. We found that the values of the critical densities and temperatures for the carbon dioxide and ethane mixtures obtained from this equation are essentially different from the values reported by Mostert [63]. Therefore we shifted the temperatures associated with the thermal conductivity data of Mostert [63] by $\Delta T = +0.260$ K at $x = 0.26$, $\Delta T = -0.478$ K at $x = 0.50$, $\Delta T = -0.445$ K at $x = 0.74$, and $\Delta T = -0.463$ K at $x = 0.75$. At the near-critical isochores for the concentrations $x = 0.74$ and $x = 0.75$ mol fraction of ethane, sharp maxima of the experimental thermal-conductivity data of Mostert and Sengers [63, 64] are observed. These maxima of the thermal conductivity are extremely narrow and sharp even in the logarithmic temperature scale, and they are observed in the one-phase region at temperatures $\tau \simeq 10^{-3}$, where all crossover functions are equal to unity. Such sharp peaks of the thermal conductivity in the one-phase region near the plait points of binary mixtures cannot be explained by the renormalization of the thermal conductivity of a binary mixture near the critical point. At these concentrations

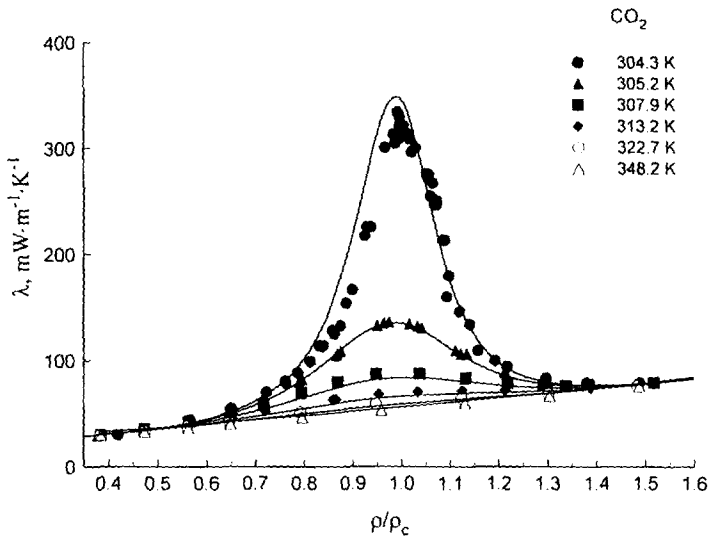

Fig. 7. The thermal conductivity of carbon dioxide as a function of the density along isotherms. The symbols indicate experimental data obtained by Michels et al. [61], and the curves represent values calculated with the crossover model.

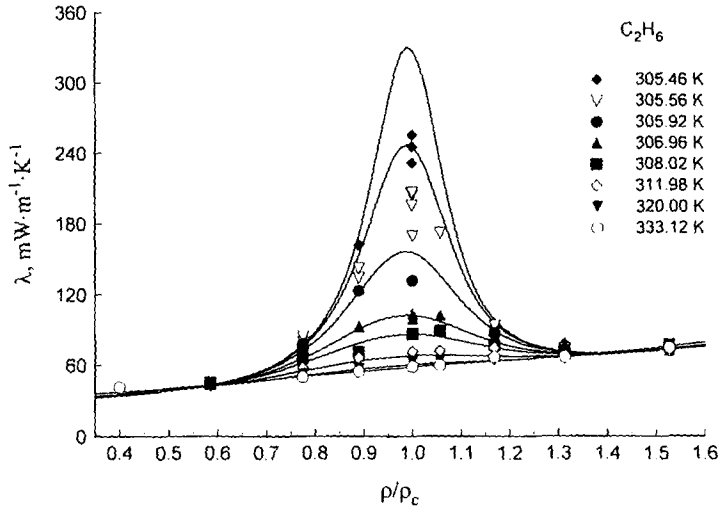

Fig. 8. The thermal conductivity of ethane as a function of the density along isotherms. The symbols indicate experimental data obtained by Mostert [63], and the curves represent values calculated with the crossover model.

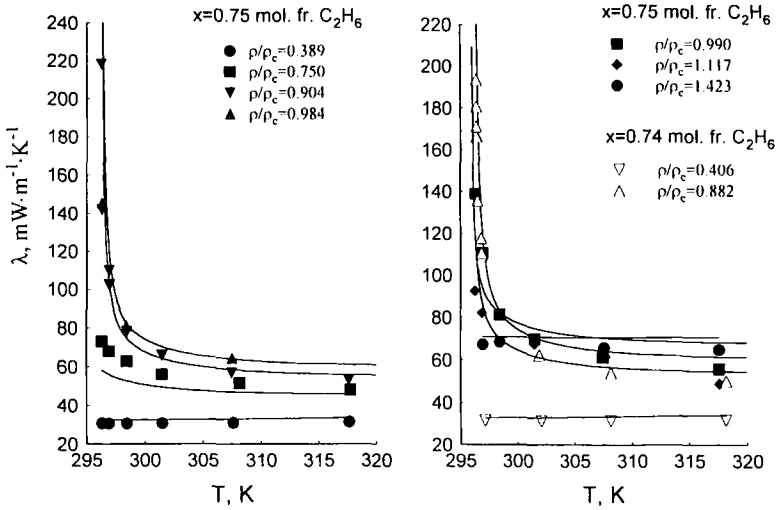

Fig. 9. The thermal conductivity of the carbon dioxide and ethane mixture at concentrations $x = 0.75$ and $x = 0.74$ mol fraction of ethane as a function of the temperature. The symbols indicate experimental data obtained by Mostert [63] and the curves represent values calculated with the crossover model.

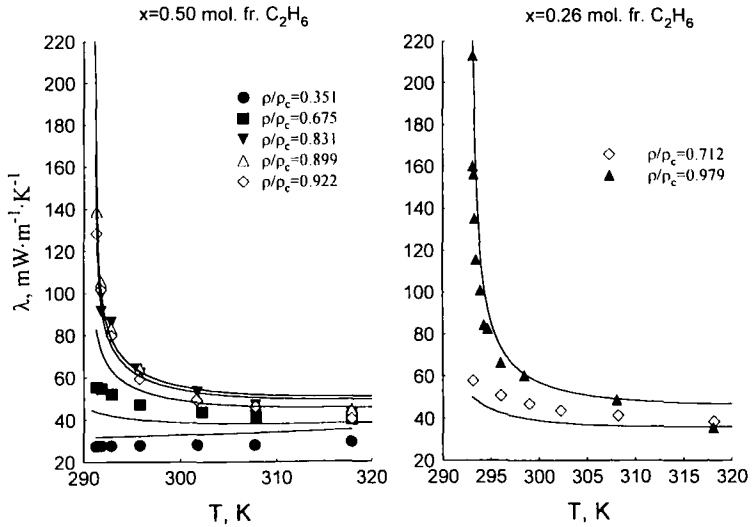

Fig. 10. The thermal conductivity of the carbon dioxide and ethane mixture at concentrations $x = 0.50$ and $x = 0.26$ mol fraction of ethane as a function of the temperature. The symbols indicate experimental data obtained by Mostert [63] and the curves represent values calculated with the crossover model.

the temperature shift arrives the value $\Delta T \cong 0.4$ K, which corresponds to the dimensionless temperature $\Delta\tau \simeq 10^{-3}$. Thus, a reasonable explanation of the experimentally observed peaks of the thermal conductivity at concentrations $x = 0.74$ and $x = 0.75$ mol fraction of ethane is that they correspond to the thermal conductivity jump in the liquid–vapor phase transition at the near-critical isochores as discussed by Luettmer-Strathmann and Sengers [21]. Therefore, we excluded from the calculations thermal-conductivity data apparently corresponding to the two-phase region. The actual thermal-conductivity values for carbon dioxide and ethane mixtures at various concentrations and densities are plotted as a function of temperature in Figs. 9 and 10. Without the two-phase region data the crossover model gives a satisfactory representation of the experimental thermal conductivity of carbon dioxide and ethane mixtures over a wide range of temperatures and densities around the critical locus. The crossover model reproduces the experimental thermal conductivity data for carbon dioxide and ethane mixtures with an accuracy comparable with the accuracy achieved for pure ethane. We have to note that our crossover model, except the coefficients γ_k, which determine the regular part of the thermal conductivity far away from the critical point, does not contain any adjustable parameters. The coefficients α_k and β_k have been found from a fit of our crossover model to the thermal-diffusion ratio data and these values have been used in further calculations; therefore, in Figs. 9 and 10 a comparison between the predictions by the crossover model values of the thermal conductivity in the critical region and the experi mental data are presented. The values of the pressure P, of the specific heat $C_{P,x}$ and of the thermal conductivity λ, calculated at some selected concentrations,

Table VI. Table for Computer Verification

Mole fraction of C_2H_6	Temperature (K)	Density ($mol \cdot L^{-3}$)	Pressure (MPa)	$C_{P,x}$ ($J \cdot g^{-1} \cdot K^{-1}$)	λ ($mW \cdot m^{-1} \cdot K^{-1}$)
0.260	293.00	9.318	6.3074	1.9275×10^5	499.5867
0.260	295.00	9.318	6.6032	3.1510×10^3	86.4668
0.260	297.00	9.318	6.9010	1.4149×10^3	67.1967
0.500	292.00	8.381	5.8098	3.4070×10^3	104.9525
0.500	295.00	8.381	6.2007	1.1509×10^3	70.3846
0.500	298.00	8.381	6.5940	6.6385×10^2	62.6211
0.740	296.00	7.600	5.3379	2.2159×10^3	416.5296
0.740	299.00	7.600	5.6818	1.0556×10^3	78.8371
0.740	302.00	7.600	6.0293	6.3908×10^2	70.0329
0.750	298.00	7.570	5.5170	1.4155×10^3	89.3309
0.750	308.00	7.570	6.6730	3.6388×10^2	64.4508

temperatures, and densities, are presented in Table VI as an aid for computer-program verification.

7. DISCUSSION

The thermodynamic and transport properties of fluids and fluid mixtures exhibit singular behavior near the critical point that cannot be described by regular equations. The asymptotic equations for the transport coefficients in binary mixtures are valid only in the near-vicinity of the critical point. In order to describe the nonasymptotic behavior of the transport properties in binary mixtures, the crossover to the regular classical behavior of the kinetic coefficients has to be considered. Simple crossover equations for these coefficients have been obtained earlier by Kiselev and Kulikov [15]. In the present paper we develop, on the basis of the decoupled-mode theory, an extended crossover model for the transport coefficients occurring in diffusion, heat conduction, and their cross-processes in fluid binary mixtures near the plait points. The crossover functions for the kinetic coefficients in a binary mixture have a simple form and coincide with the crossover function for the thermal conductivity in the one-component limit.

The crossover equations for the thermal-conductivity and the thermal diffusion ratio in binary mixtures near the vapor–liquid critical line have been considered. The crossover behavior of the transport coefficients of a binary mixture along the critical isochore is determined by the characteristic temperature τ_D. In the temperature range $\tau_D \ll \tau \ll 1$ the thermal conductivity of a binary mixture behaves as the thermal conductivity of a pure fluid. Asymptotically close to the critical point at $\tau \ll \tau_D$ the thermal conductivity of a binary mixture is renormalized and, unlike the thermal conductivity of a pure fluid, does not diverge and tends to its critical background value in the critical point. At temperatures $\tau \simeq \tau_D$ the thermal conductivity of binary mixtures is a monotonic function of the temperature and exhibits a crossover from one-component-like behavior to the critical background. These predictions for the thermal conductivity are consistent with the results of a theoretical analysis performed earlier by Onuki [6]. Our estimates of the value of the characteristic temperature τ_D with Eq. (56) give that, for carbon dioxide and ethane mixtures, $\tau_D = 8.2 \times 10^{-9}$ at $x = 0.26$ (azeotropic mixture), $\tau_D = 1.7 \times 10^{-6}$ at $x = 0.40$, $\tau_D = 1.2 \times 10^{-5}$ at $x = 0.50$, and $\tau_D = 6.3 \times 10^{-5}$ at $x = 0.75$. This means that in the critical region at temperatures 10^{-6}–$10^{-5} < \tau \ll 1$ the thermal conductivity of carbon dioxide and ethane mixtures exhibits a one-component-like behavior (57). The renormalization of the thermal conductivity described by Eq. (58) and the renormalization of the thermal-diffusion

ratio as given by Eq. (65) in these mixtures can be observed only at temperatures $\tau \ll 10^{-6}$, which makes it very complicated for experimental observation. We applied our crossover model to a description of the experimental thermal-diffusion ratio data of Walther [58] for the carbon dioxide and ethane mixture and the experimental thermal-conductivity data obtained by Mostert [63]. The results of our calculations for the thermal conductivity (see Figs. 9 and 10) confirm this theoretical conclusion. An asymptotic temperature behavior of the thermal-diffusion ratio calculated with the crossover equation, Eq. (63), along the critical isochores at composition $x = 0.4$ mol fraction of ethane mixtures is shown in Fig. 11. The renormalization of Eq. (58) for the thermal-diffusion ratio is really observed at temperatures $\tau \ll 10^{-6}$.

It is also interesting to compare the result of our calculations for carbon dioxide and ethane mixtures with the results obtained by Luettmer-Strathmann and Sengers [21]. In our approach the crossover function $\Omega_{cS} \equiv 0$, which corresponds to the direct calculations of Luettmer-Strathmann and Sengers [21]. A comparison between our crossover functions Ω_x and Ω and the corresponding crossover functions Ω_{cc} and Ω_{SS} introduced by Luettmer-Strathmann and Sengers [21] is shown in Fig. 12.

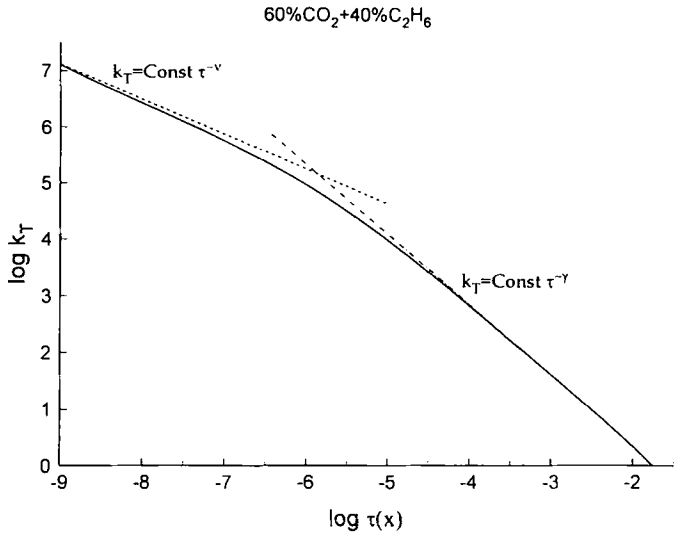

Fig. 11. The thermal-diffusion ratio of the carbon dioxide and ethane mixture as a function of temperature along the critical isochore at the concentration $x = 0.4$ mol fraction of ethane. The solid curve represents the values calculated with the crossover model, the dashed curve corresponds to the asymptotic behavior at $\tau \ll \tau_D$, and the dotted–dashed curve corresponds to the asymptotic behavior at $\tau_D \ll \tau \ll 1$.

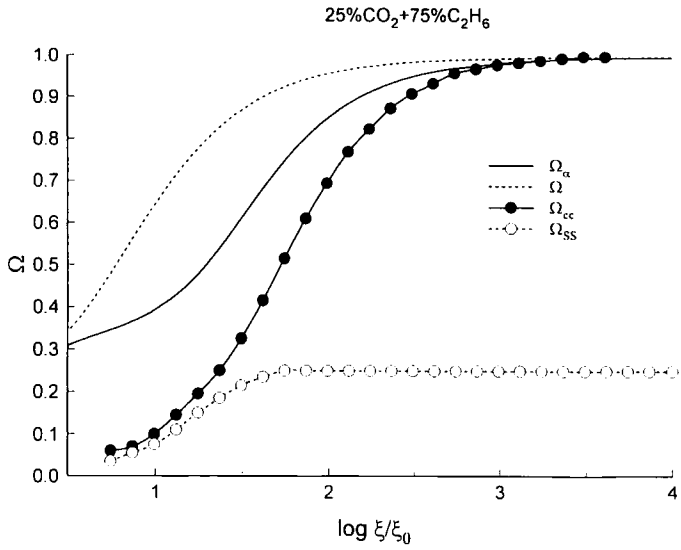

Fig. 12. The crossover functions for the transport Coefficients of the carbon dioxide and ethane mixture at concentration $x = 0.75$ mol fraction of ethane as a function of the dimensionless correlation length along the critical isochore.

The functions Ω_α and Ω_{cc} exhibit qualitatively the same behavior; however, the crossover function Ω_{SS}, unlike our crossover function Ω, does not tend to unity in the asymptotic critical region, but $\Omega_{SS} \to 0.25$ at $\xi \to \infty$ ($\tau \to 0$).

Quantitatively the calculations of Luettmer-Strathmann and Sengers [21] for carbon dioxide and ethane mixtures give a slightly better representation of the thermal conductivity at separate isochores far away from the critical point. In order to describe the thermal-conductivity surface of binary mixtures in a wide region around the critical locus better, we have to use more coefficients in Eqs. (89), (90), and (103) than we used in the present paper. However, for that purpose we need more detailed experimental data for the thermal conductivity and diffusion coefficients of carbon dioxide and ethane mixtures.

APPENDIX

Our aim is to obtain a crossover expression for the kinetic coefficient $\tilde{\alpha}$ with account of the next term $\propto k^4$ in the effective Hamiltonian of the system. With this in mind, we consider the Hamiltonian in the form

$$H = \tfrac{1}{2} \int (a\tau\varphi^2 + c(\nabla\varphi)^2 + c_1^2(\Delta\varphi)^2)\, d\vec{r} = \tfrac{1}{2} \sum_{\vec{k}} (a\tau + ck^2 + c_1^2 k^4)\, |\varphi_{\vec{k}}|^2 \quad \text{(A.1)}$$

The static correlation function in this case reads

$$G(\vec{k}) = \langle |\varphi_{\vec{k}}|^2 \rangle = \frac{k_B T}{a\tau + ck^2 + c_1^2 k^4} = \frac{k_B T (\partial x/\partial \mu)_{P,T}}{\rho[1+(k\xi)^2][1+(kl)^2]} \quad \text{(A.2)}$$

where the correlation length in this approximation is given by

$$\xi^2 = \frac{\xi_{OZ}^2}{2}(1 + \sqrt{1 - 4(l_0/\xi_{OZ})^2}) \quad \text{(A.3)}$$

and

$$l^2 = \frac{\xi_{OZ}^2}{2}(1 - \sqrt{1 - 4(l_0/\xi_{OZ})^2}) \quad \text{(A.4)}$$

is a new noncritical size which remains finite at the critical point ($l \to l_0$ at $\xi_{OZ} \to \infty$). Here $l_0^2 = c_1^2/c_0$, and $\xi_{OZ} = \sqrt{c\rho^{-1}(\partial x/\partial \mu)_{P,T}}$ is the Ornstein–Zernike correlation length. Substitution of Eq. (A.2) into Eq. (19) and integration over all k up to the cutoff wave number q_D yield

$$\Delta\tilde{\alpha} = \frac{k_B T \rho}{6\pi\eta} \frac{(\partial x/\partial \mu)_{P,T}}{\xi(1-(l/\xi)^2)} \Omega_\alpha^{(1)}(q_D, \xi, l) \quad \text{(A.5)}$$

where the new crossover function

$$\Omega_\alpha^{(1)}(q_D, \xi, l) = \frac{2}{\pi}\{\arctan(q_D\xi) - (l/\xi)\arctan(q_D l) + \Omega_\alpha^{(2)}(q_D, \xi, l)\} \quad \text{(A.6)}$$

with

$$\Omega_\alpha^{(2)}(q_D, \xi, l) = \frac{\sqrt{2}\,l}{F}\left[\frac{1}{\sqrt{\xi^2 + l^2 + (\xi^2 - l^2)F}} \arctan \frac{\sqrt{2}\,q_D \xi l}{\sqrt{\xi^2 + l^2 + (\xi^2 - l^2)F}} - \frac{1}{\sqrt{\xi^2 + l^2 - (\xi^2 - l^2)F}} \arctan \frac{\sqrt{2}\,q_D \xi l}{\sqrt{\xi^2 + l^2 - (\xi^2 - l^2)F}}\right] \quad \text{(A.7)}$$

and

$$F = \sqrt{1 - \frac{4y_D q_D l^2 \xi^2 (l + \xi)}{(\xi^2 - l^2)^2}} \quad \text{(A.8)}$$

The validity of these expressions is restricted by the obvious condition $F^2 \geqslant 0$ or, equivalently,

$$(\xi^2 - l^2)^2 - 4y_D q_D l^2 \xi^2 (l + \xi) \geqslant 0 \tag{A.9}$$

A solution of this inequality with the reasonable estimates $y_D \simeq 1$, $l \simeq l_0$, and $q_D l_0 \simeq 1$ gives $(l/\xi) \leqslant 0.2$. In this region we can replace the function F on its expansion in powers of the small parameter (l/ξ):

$$F \cong 1 - 2y_D q_D l(l/\xi) + \mathcal{O}(l^2/\xi^2) \tag{A.10}$$

and consider the correlation length ξ and the noncritical size l in the critical limit only ($\xi = \xi_{OZ}$, $l = l_0$). Then Eq. (A.7) for the crossover function $\Omega_\alpha^{(1)}$ reduces to

$$\begin{aligned}\Omega_\alpha^{(2)}(q_D, \xi, l) = {} & \frac{(l/\xi_{OZ})}{\sqrt{1 - y_D q_D \hat{\xi}(l/\xi_{OZ})^2}} \arctan \frac{q_D l}{\sqrt{1 - y_D q_D \hat{\xi}(l/\xi_{OZ})^2}} \\ & - \frac{1}{\sqrt{1 + y_D q_D \hat{\xi}}} \arctan \frac{q_D \xi}{\sqrt{1 + y_D q_D \hat{\xi}}} \\ \cong {} & \frac{l}{\xi_{OZ}} \arctan(q_D l) - \frac{1}{\sqrt{1 + y_D q_D \hat{\xi}}} \arctan \frac{q_D \xi_{OZ}}{\sqrt{1 + y_D q_D \hat{\xi}}} \\ & + \mathcal{O}(l^3/\xi^3)\end{aligned} \tag{A.11}$$

with renormalized correlation length,

$$\hat{\xi} = \xi_{OZ}\left(1 - \left(\frac{l_0}{\xi_{OZ}}\right)^2\right) \tag{A.12}$$

Substituting Eq. (A.11) into Eq. (A.6) gives

$$\Omega_\alpha^{(1)}(q_D \hat{\xi}) = \frac{2}{\pi}\left\{\arctan(q_D \xi_{OZ}) - \frac{1}{\sqrt{1 + y_D q_D \hat{\xi}}} \arctan \frac{q_D \xi_{OZ}}{\sqrt{1 + y_D q_D \hat{\xi}}}\right\} \tag{A.13}$$

Equation (A.13) was obtained under the condition $(l/\hat{\xi}) \ll 1$; however, unlike Eqs. (A.6)–(A.8), it can be extrapolated also in the region where $(l/\hat{\xi}) \gg 1$. As one can see from Eq. (A.13), far away from the critical point $\xi_{OZ} \simeq l_0$, $\hat{\xi} \to 0$, and the crossover function $\Omega_\alpha^{(1)} \to 0$. If we demand that not only the crossover function $\Omega_\alpha^{(1)}$ but also its first derivative tends to

zero in this region, we can replace ξ_{OZ} in Eq. (A.13) by the renormalized correlation length $\hat{\xi}$. This replacement does not change the crossover function in the critical region where $\xi_{OZ} \simeq \hat{\xi}$ and provides the correct asymptotic of this function in the case $\xi_{OZ} \simeq l_0$. Finally, Eqs. (A.5) and (A.6) can be written in the form

$$\Delta\tilde{\alpha} = \frac{k_B T \rho (\partial x/\partial \mu)_{P,T}}{6\pi\eta\hat{\xi}} \Omega_x^{(1)}(q_D\hat{\xi}) \tag{A.14}$$

with

$$\Omega_x^{(1)}(q_D\hat{\xi}) = \frac{2}{\pi}\left\{\arctan(q_D\hat{\xi}) - \frac{1}{\sqrt{1+y_D q_D\hat{\xi}}}\arctan\frac{q_D\hat{\xi}}{\sqrt{1+y_D q_D\hat{\xi}}}\right\} \tag{A.15}$$

One can see that Eqs. (A.14) and (A.15) coincide with Eqs. (23) and (27), respectively, with account of the replacement ξ by the renormalized correlation length $\hat{\xi}$.

ACKNOWLEDGMENTS

The authors are indebted to J. W. Magee, J. C. Rainwater, and J. V. Sengers for valuable discussions. One of us (S.B.K.) acknowledges the hospitality of the Physical and Chemical Properties Division of the National Institute of Standards and Technology in Boulder, CO, where this paper was prepared. The research was supported by the Russian Fund for Basic Research under Grant 94-02-03555.

REFERENCES

1. L. D. Landau and E. M. Lifshitz, *Statistical Physics* 3rd ed. (Pergamon, New York, 1980).
2. A. Z. Patashinskii and V. L. Pokrovskii, *Fluctuation Theory of Phase Transitions* (Pergamon, New York, 1979).
3. E. E. Gorodetskii and M. S. Giterman, *Sov. Phys. JETP* **30**:348 (1970).
4. L. Mistura, *Nuovo Cimento* **12B**:35 (1972).
5. L. Mistura, *J. Chem. Phys.* **62**:4571 (1975).
6. A. Onuki, *J. Low Temp. Phys.* **61**:101 (1985).
7. M. A. Anisimov and S. B. Kiselev, *Int. J. Thermophys.* **13**:873 (1992).
8. Z. Y. Chen, A. Abbaci, S. Tang, and J. V. Sengers, *Phys. Rev. A* **42**:4470 (1990).
9. M. A. Anisimov, S. B. Kiselev, J. V. Sengers, and S. Tang, *Physica A* **188**:487 (1992).
10. S. B. Kiselev and J. V. Sengers, *Int. J. Thermophys.* **14**:1 (1993).
11. J. K. Bhattacharjee, R. A. Ferrell, R. S. Basu, and J. V. Sengers, *Phys. Rev. A* **24**:1469 (1981).
12. G. A. Olchowy and J. V. Sengers, *Phys. Rev. Lett.* **61**:15 (1988).
13. G. A. Olchowy and J. V. Sengers, *Int. J. Thermophys.* **10**:417 (1989).

14. J. Luettmer-Strathmann, J. V. Sengers, and G. A. Olchowy, *J. Chem. Phys.* **103**:7482 (1995).
15. S. B. Kiselev and V. D. Kulikov, *Int. J. Thermophys.* **15**:283 (1994).
16. S. B. Kiselev and A. A. Povodyrev, in *Proceedings of the 4th Asian Thermophysical Properties Conference, Vol. 1*, A. Nagashima, ed. (Keio University, Tokyo, 1995), p. 699.
17. S. B. Kiselev and A. A. Povodyrev, *High Temp.* **34**:621 (1996).
18. R. Folk and G. Moser, *J. Low Temp. Phys.* **99**:11 (1995).
19. R. Folk and G. Moser, *Int. J. Thermophys.* **75**:2706 (1995).
20. R. Folk and G. Moser, *Phys. Rev. Lett.* **16**:1363 (1995).
21. J. Luettmer-Strathmann and J. V. Sengers, *J. Chem. Phys.* **104**:3026 (1996).
22. G. X. Jin, S. Tang, and J. V. Sengers, *Phys. Rev. E* **47**:388 (1993).
23. G. X. Jin, *Effects of Critical Fluctuations of the Thermodynamic Properties of Fluids and Fluid Mixtures*, Ph.D. thesis (University of Maryland, 1993).
24. J. W. Magee, *J. Chem. Eng. Data* **40**:438 (1995).
25. W.-W. R. Lau, *A Continuously Weighed Pyncometer Providing Densities for Carbon Dioxide + Ethane Mixtures Between 240 and 350 K and Pressures Up to 35 MPa*, Ph.D. thesis (Texas A & M University, College Station, 1986).
26. S. B. Kiselev, *Fluid Phase Equil.* **128**:1 (1997).
27. R. A. Ferrell, *Phys. Rev. Lett.* **24**:1169 (1970).
28. L. D. Landau and E. M. Lifshitz, *Hydrodynamics* (Nauka, Moscow, 1988).
29. R. Perl and R. A. Ferrell, *Phys. Rev. A* **6**:2358 (1972).
30. K. Kawasaki, in *Phase Transition and Critical Phenomena, Vol. 5A*, C. Domb and M. S. Green, eds. (Academic Press, New York, 1976), p. 165.
31. K. Kawasaki, *Ann. Phys.* **61**:1 (1970).
32. L. P. Kadanoff and J. Swift, *Phys. Rev.* **166**:89 (1968).
33. E. D. Siggia, B. I. Halperin, and P. C. Hohenberg, *Phys. Rev. B* **13**:2110 (1976).
34. J. M. H. Levelt Sengers and J. V. Sengers, in *Perspectives in Statistical Physics*, H. J. Raveche, ed. (North-Holland, Amsterdam, 1981), p. 239.
35. M. A. Anisimov and S. B. Kiselev, *Sov. Tech. Rev. Ser. B. Therm. Phys.* **3**(2) (Harwood Academic, Chur-Melbourne, 1992).
36. S. S. Leung and R. B. Griffiths, *Phys. Rev. A* **8**:2673 (1973).
37. S. B. Kiselev and A. A. Povodyrev, *Fluid Phase Equil.* **79**:33 (1992).
38. W. Duschek, R. Kleinrahm, and W. Wagner, *J. Chem. Thermodyn.* **22**:827 (1990); **22**:841 (1990).
39. R. Gilgen, R. Kleinrahm, and W. Wagner, *J. Chem. Thermodyn.* **24**:1243 (1992).
40. A. Michels and C. Michels, *Proc. Roy. Soc. Lond. Ser. A* **153**:201 (1936).
41. J. C. Holste, K. R. Hall, P. T. Eubank, G. Esper, M. Q. Watson, W. Warowny, D. M. Bailey, J. G. Young, and M. T. Bellomy, *J. Chem. Thermodyn.* **19**:1233 (1987).
42. A. Fenghour, W. A. Wakeham, and J. T. R. Watson, *J. Chem. Thermodyn.* **27**:219 (1995).
43. J. W. Magee and J. F. Ely, *Int. J. Thermophys.* **7**:1063 (1986).
44. L. A. Weber, *Int. J. Thermophys.* **13**:1011 (1992).
45. A. Fredenslund and J. Mollerup, *J. Chem. Soc. Faraday Inst.* **70**:1653 (1974).
46. D. G. Friend, *NIST Mixture Property Program*, NIST14, Version 9.08 (National Institute of Standards and Technology, Gaithersburg, MD, 1992).
47. K. Ohgaki and T. Katayama, *Fluid Phase Equil.* **1**:27 (1992).
48. T. S. Brown, A. J. Kidnay, and E. D. Sloan, *Fluid Phase Equil.* **40**:169 (1988).
49. M. S.-W. Wei, T. S. Brown, A. J. Kidnay, and E. D. Sloan, *J. Chem. Eng. Data* **40**:726 (1995).
50. J. M. Prausnitz and R. D. Gunn, *AIChE J.* **4**:430 (1958); **4**:498 (1958).
51. R. D. Gunn *AIChE J.* **18**:183 (1972).

52. J. V. Sengers and P. H. Keyes, *Phys. Rev. Lett.* **26**:70 (1971).
53. J. H. Ferziger and H. G. Kaper, *Mathematical Theory of Transport Processes in Gases* (North-Holland, Amsterdam, 1972).
54. E. N. Fuller and J. C. Giddings, *J. Gas. Chromotogr.* **3**:222 (1965).
55. E. N. Fuller, P. D. Schettler, and J. C. Giddings, *Ind. Eng. Chem.* **58**(5):18 (1966).
56. J. Leffler and H. T. Gullinan, *Ind. Eng. Chem. Fundam.* **9**:84 (1970); **9**:88 (1970).
57. M. A. Lusis and G. A. Ratcliff, *Can. J. Chem. Eng.* **46**:385 (1968).
58. J. E. Walther, *Thermal Diffusion in Non-Ideal Gases*, Ph.D. thesis (University of Illinois, 1957).
59. A. Wassilijeva, *Phys. Z* **5**:737 (1894).
60. A. L. Lindsay and L. A. Bromley, *Ind. Eng. Chem.* **42**:1508 (1950).
61. A. Michels, J. V. Sengers, and P. S. van der Gulik, *Physica* **28**:1216 (1962).
62. R. Mostert, H. R. van der Berg, P. S. van der Gulik, and J. V. Sengers, *J. Chem. Phys.* **92**:5454 (1990).
63. R. Mostert, *The Thermal Conductivity of Ethane and Its Mixtures with Carbon Dioxide in the Critical Region*, Ph.D. thesis (University of Amsterdam, Amsterdam, 1992).
64. R. Mostert and J. V. Sengers, *Fluid Phase Equil.* **75**:235 (1992).
65. H. Preston-Thomas, *Metrologia* **27**:3 (1992).